Journal of Alloys and Compounds 882 (2021) 160774

Contents lists available at ScienceDirect

Journal of Alloys and Compounds

journal homepage: www.elsevier.com/locate/jalcom

Review

Current state of high voltage olivine structured $LiMPO_4$ cathode materials for energy storage applications: A review

Nurbol Tolganbek[a], Yerkezhan Yerkinbekova[a,b], Sandugash Kalybekkyzy[b], Zhumabay Bakenov[a,b,*], Almagul Mentbayeva[a,b,*]

[a] Department of Chemical and Materials Engineering, School of Engineering and Digital Sciences, Nazarbayev University, Kabanbay Batyr Ave. 53, Nur-Sultan 010000, Kazakhstan
[b] National Laboratory Astana, Nazarbayev University, Kabanbay Batyr Ave. 53, Nur-Sultan 010000, Kazakhstan

ARTICLE INFO

Article history:
Received 29 April 2021
Received in revised form 3 June 2021
Accepted 7 June 2021
Available online 10 June 2021

Keywords:
Lithium-ion battery
Olivine
High voltage cathode
$LiCoPO_4$
$LiNiPO_4$

ABSTRACT

Continuous evolution of electrode materials still has not correspond today's energy storage system necessity and limits their application range. Numerous approaches are proposed to improve lithium ion batteries (LIBs) energy density including advancement of positive electrode materials. Olivine structured cathodes as $LiCoPO_4$ and $LiNiPO_4$ are excellent candidates due to their working potentials of exceeding 5.0 V vs. Li^+/Li. Despite the efforts, these materials still have several intrinsic problems which demand various strategies to overcome. The paper systematically reviews the recent progress of these cathode materials. The approaches based on particle size manipulation via synthesis route variation and carbon addition, surface modification by coating with electron conducting carbon layer, and doping the structure with other metal ions were discussed and analyzed as the most impactful towards achieving competitive performance. Furthermore, the computational technique was discussed due to its importance in understanding and designing the materials from atomic to microscale levels. The potential applications of these cathodes in a new generation of all-solid-state Li-ion and aqueous batteries were described.

Contents

1. Introduction

Owing to their highest energy density, lithium-ion batteries (LIBs) are the most widely applied energy storage systems among commercially available rechargeable batteries. Further improvement of their performance is demanded by emerging technologies, which require higher operating voltage/energy density, stability and prolonged operation. These developments depend on advancement of every component of battery systems such as anode, cathode, electrolyte, separator and, etc [1,2]. Particularly, a high energy density is gained by either high specific capacity or operating potential of a positive electrode [3,4]. In the market, there are several types of

* Corresponding author at: National Laboratory Astana, Nazarbayev University, Kabanbay Batyr Ave. 53, Nur-Sultan 010000, Kazakhstan.

https://doi.org/10.1016/j.jallcom.2021.160774
0925-8388/

Table 1
The summary of commercial cathode materials with major electrochemical characteristics.

Cathode materials	Structure type	Potential vs Li/Li^+, V	Theoretical capacity, mAh g^{-1}
$LiMO_2$	Layered		
$LiCoO_2$		3.7	274
$LiMnO_2$			285
$LiNiO_2$			
$LiNi_{1-x-y}Co_xM_yO_2$	Layered		
$LiNi_{1-x-y}Co_xAl_yO_2$, NCA		~ 4.4	195
$LiNi_{1-x-y}Co_xMn_yO_2$, NCM		~ 4.5	200
$LiMn_2O_4$	Spinel	4.0	148
$LiMPO_4$	Olivine		
$LiFePO_4$		3.5	170
$LiMnPO_4$		4.1	170
$LiCoPO_4$		4.8	167
$LiNiPO_4$		5.2	170

commercialized cathode materials, namely lithium metal oxides ($LiMO_2$) [5–10] and their doping derivatives ($LiNi_xCo_yAl_{1-x-y}O_2$, NCA [11,12] and $LiNi_xMn_yCo_zO_2$, NMC) [13,14] and lithium iron phosphate ($LiFePO_4$, LFP) [15,16], shown in Table 1 and Fig. 1.

The oxide-based materials with a layered structure, especially $LiCoO_2$ are widely consumed cathodes in lithium-ion cells. Having one of the highest theoretical capacity of 274 mAh g^{-1}, the material suffers with providing only a half of it, because of impossibility to extract all lithium ions during the charging process. In addition to this, among other members of this family lithium manganese-oxide has low electronic conductivity, while $LiNiO_2$ is difficult to synthesize in pure phase [18]. Doped derivatives of $LiNiO_2$ known as nickel-rich oxide cathodes such as NCA and NCM have gained a significant amount of attention due to the high-energy density [11,12]. Again, obtaining practical capacity close to the theoretical one is difficult because of insufficient electrochemical durability [13,14] (Fig. 2a). Another available cathode material is spinel structured $LiMn_2O_4$, that has a theoretical capacity of 148 mAh g^{-1}, however, in the practice only 120 mAh g^{-1} can be reached. The lower practical capacity of spinel cathodes restricts the energy density of Li-ion batteries. There is another disadvantage of the manganese consumption in the cathode materials due to the reduction nature of the metal. A currently known cathode with high charging and discharging efficiency is olivine structured LFP [19] that has the theoretical capacity of 170 mAh g^{-1} with 97–98% of retention over 1000 cycles.

Addition to the practical capacity (Fig. 2b) of almost as the theoretical one the materials also have long cycle life due to the olivine structure, which enables full extraction and insertion of lithium ions during lithiation and delithiation processes.

One of the main disadvantages of LFP implementation into electric and hybrid vehicles (EV, HV) is a limited nominal potential of 3.2 V [20,21]. Gaining more power with a smaller battery package for high-voltage battery system could be possible only with high potential cathodes. Beneficially, having the same theoretical capacity as LFP, other cathodes from olivine family recently have gained a significant amount of attention due to their higher working potential of 4.8 and 5.2 V vs Li/Li^+ for $LiCoPO_4$ (LCP) [22–26] and $LiNiPO_4$ (LNP) [25–38], respectively. Typical cyclic voltammetry (CV) profiles of LCP and LNP are shown in Fig. 3. The high applicable candidacy of these olivine materials is also due to low cost, availability in a large amount, reduced volume expansion, relatively high specific capacity.

In the olivine structure, a MO_6 octahedron joins with edges of two LiO_6 octahedra and one PO_4 tetrahedron [40]. The ion diffusion within crystal occurs in 1D pathway (010) (Fig. 4b) [41], a direction which hinders the fast ion insertion and extraction because of separation of MO_6 octahedra and LiO_6 tetrahedra polyanions [42,43]. The ordered olivine structure of $LiMPO_4$ is obtained with transition d-metals such as iron (Fe), manganese (Mn), cobalt (Co), and nickel (Ni) [41,44] (Fig. 2b).

Generally, the olivine structure has a formula of M_2XO_4, where M atoms are partially in the octahedral sites while X atoms in 1/8 of a tetrahedral occupancies of a hexagonal close-packed oxygen matrix (Fig. 4a, [45]). Octahedral sites in olivine structure crystallographically differ from each other in size, thus the formula is $M'MPO_4$ [46,47]. Metal ions in such systems could be different in size and charge. Further, this system was adapted for energy application systems. The first olivine structured cathode material was prepared and reported by J. Goodenough in 1997 [45].

Despite having superior safety, great reversibility, high operating potentials, wide energy density and capacity for high power applications, the consumption of olivine structured cathodes have a few unsolved technical objections such as poor cycle stability and rate performance [40,42,48]. Some of the drawbacks of these materials can be improved by decreasing particle size [39,40,42,44,51], doping by other d-elements [40,41] and coating with carbon [48–55]. Besides these, the surface modification prevents degradation of cathodes by avoiding direct contact with organic electrolyte, as they can react with HF – a product of electrolyte decomposition [56,57]. All these undesired side reactions may lead to capacity decay and poor

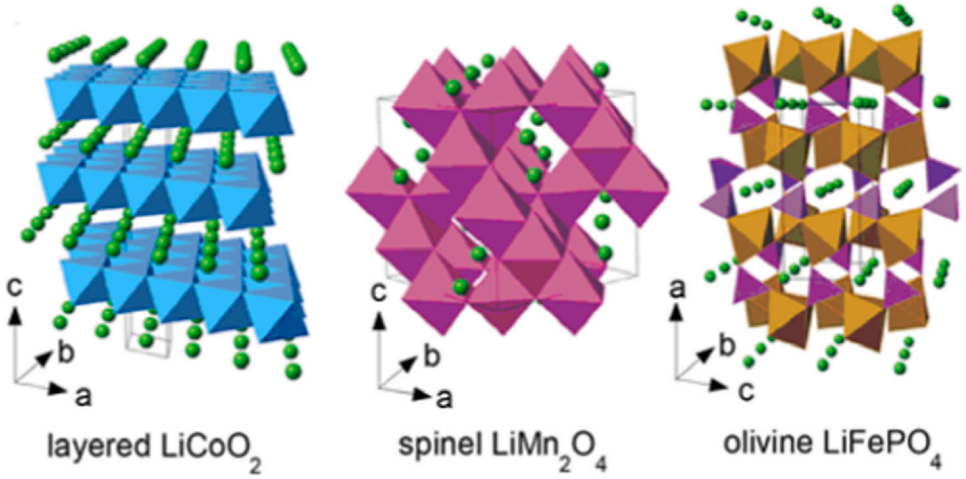

Fig. 1. The crystal structure of three different types of cathode materials [17].

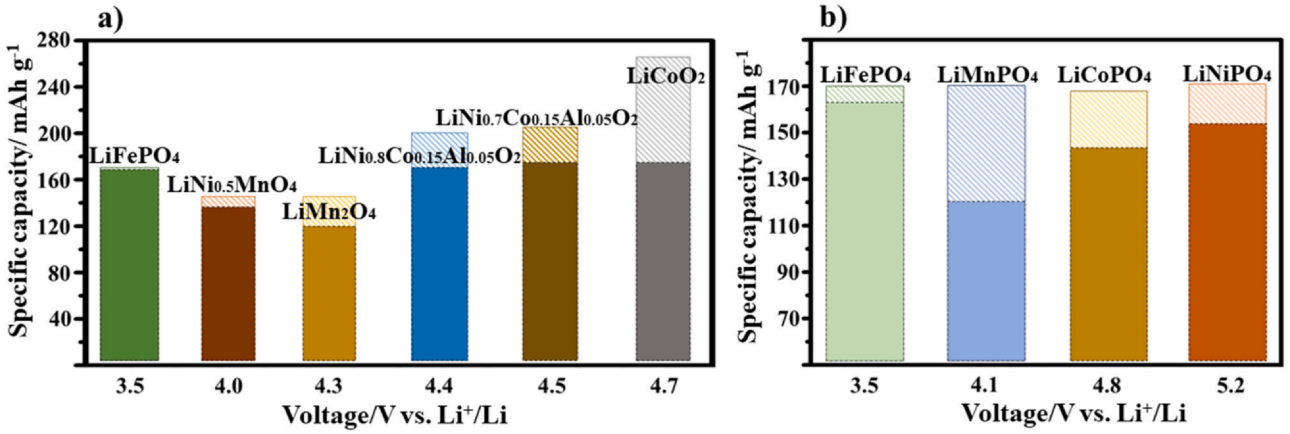

Fig. 2. Specific capacity vs. potential of some commercial (a) and olivine structured (b) cathodes. Saturated colors represent practical capacity of cathodes, and pattern filled columns are theoretical capacity.

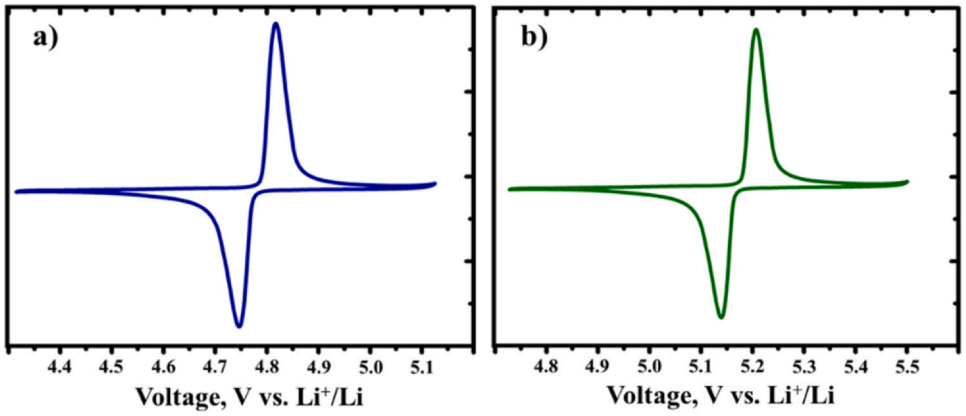

Fig. 3. CV profiles of olivine cathodes: LCP (a) and LNP (b).

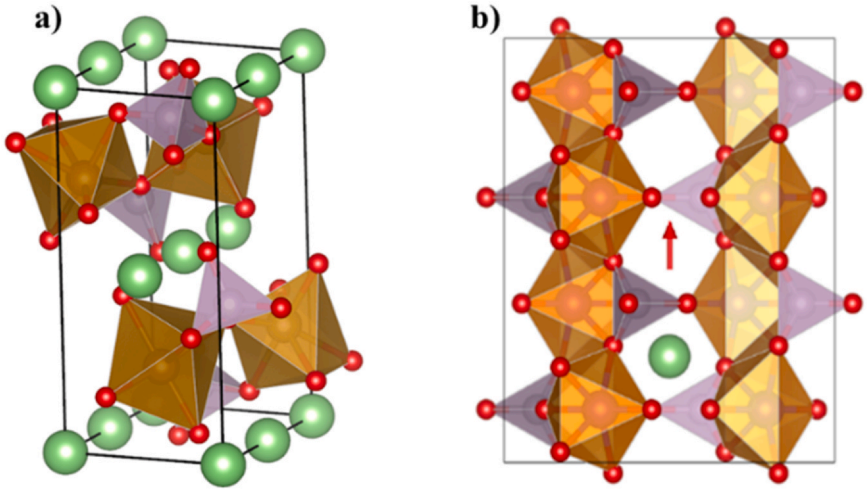

Fig. 4. Crystal structure of olivine; brown colored polyhedral are MO_6; purples are PO_4; red ones are oxygen atom while greens are lithium ions [40] (a). Li-ion diffusion in 1-dimensional pathway of olivine structure (b) [41].

cyclability of the electrodes. Regardless of the above-mentioned complications the progress of high voltage olivine cathodes is one of the main targets for current storage systems, because they can store substantially more energy than conventional cathode materials and provide opportunities for a mass production of EV. Therefore, $LiCoPO_4$ and $LiNiPO_4$ are promising cathodes for LIBs. Recently, many efforts on improving these two components have taken the research to another level with favorable outcomes as expectations have been greater. In 2018 Hector et al. summarized development of olivine $LiCoPO_4$ cathode material, comparing its preparation methods, structure and performance [58]. Review work on $LiNiPO_4$ cathode is also necessary since there is a large amount of research work on its

preparation and applications. Thus, a summary work for these cathodes is crucial and required to cover the most recent advancements.

*I*n this review paper, the concentration will be on high voltage operating olivine structured $LiMPO_4$ cathode materials based on transition metals like cobalt (Co) and nickel (Ni). The paper includes the latest advances regarding a particle manipulation through synthesizing methods, surface modification via carbon coating, and a partial substitution of Co and Ni by other transition D-elements. The quantum mechanical calculations are also presented to discuss the insight investigations and suggestions for enhancing the performance of the materials. The future perspectives of these cathodes in the field of all-solid-state (ASSB) and aqueous batteries are discussed.

2. Particle size manipulation

The particle size is a key factor on the electrochemical reactivity of olivine-structured materials. Findings indicated that reducing particles size of $LiCoPO_4$/$LiNiPO_4$ to nanometers can influence on electrochemical characteristics of the cathode by shortening the diffusion distance for Li ions during the charge–discharge process [58]. Furthermore, nanoscale sizing should enhance the rate capability and obtain high discharge capacity, as well as decrease structural degradation and deformation of cathodes during cycling [59]. Therefore, this section describes the effect of particle size manipulation.

The size of LCP/LNP cathodes are mainly controlled via fabrication methods. Various synthesizing routes such as solvothermal [60,61], hydrothermal [62,63], sol-gel [64,65], solid-state [66,67], co-precipitation [68], spray pyrolysis [69], supercritical fluid [70,71] process and other combined preparation methods [72,73] can be used to obtain smaller particles. Solvothermal synthesis method allowed to produce a well-controlled morphology and particle size of LCP. Recently, an investigation found that a solvent played a crucial role in adjusting the size of crystals [74,75]. Particularly, solvent such as ethylene glycol (EG) that had a high viscosity was able to control the growth of LCP crystals [76]. EG was similar to those of water, such as small molecules and the ability to form networks of hydrogen bonds [73]. In addition, the high dielectric constant of EG enabled dissolving highly polar reaction compounds, while the strong chelating ability allowed it to easily form complexes with transition metal ions in solution. Thus, EG content in the mixed solvent significantly affected the solubility, reactivity and diffusion behavior of the reagents and effectively controlled the morphology and size of the final product [76]. Wu et al. stated that adjusting the water/ethylene glycol ratio can effectively control the particle size of LCP in solvothermal synthesis [60]. The powders from the method had a particle size of 500 nm which demonstrated an initial discharge capacity of 124 mAh g^{-1} at 0.1 C, and capacity retention remained at 83% after 100 cycles. Another study observed that diethylene glycol played an essential role in changing the particle size [62]. Using water/diethylene glycol with the ratio of 1: 6 (v/v) enabled obtaining powder with a uniform particle size of ~ 150 nm as shown in Fig. 5. The cathode after heating in argon (Ar) exhibited high initial discharge capacity of 147 mAh g^{-1} at 0.1 C with a capacity retention of 70% after 40 cycles. Neef et al. synthesized plate-like shaped LCP with thickness of about 200 nm that had arranged flower-like structure. Outcome of the research demonstrated that adding organic compounds during the hydrothermal method to produce desired form positively influenced on electrochemical performance (107 mAh g^{-1}) [62].

A favorable fabrication method that enabled precise control of the morphology and particle size was a sol-gel. Kim et al. were able to fabricate a single phase porous sponge-like $LiCoPO_4$ without any secondary phase or impurities through a sol-gel route [64].

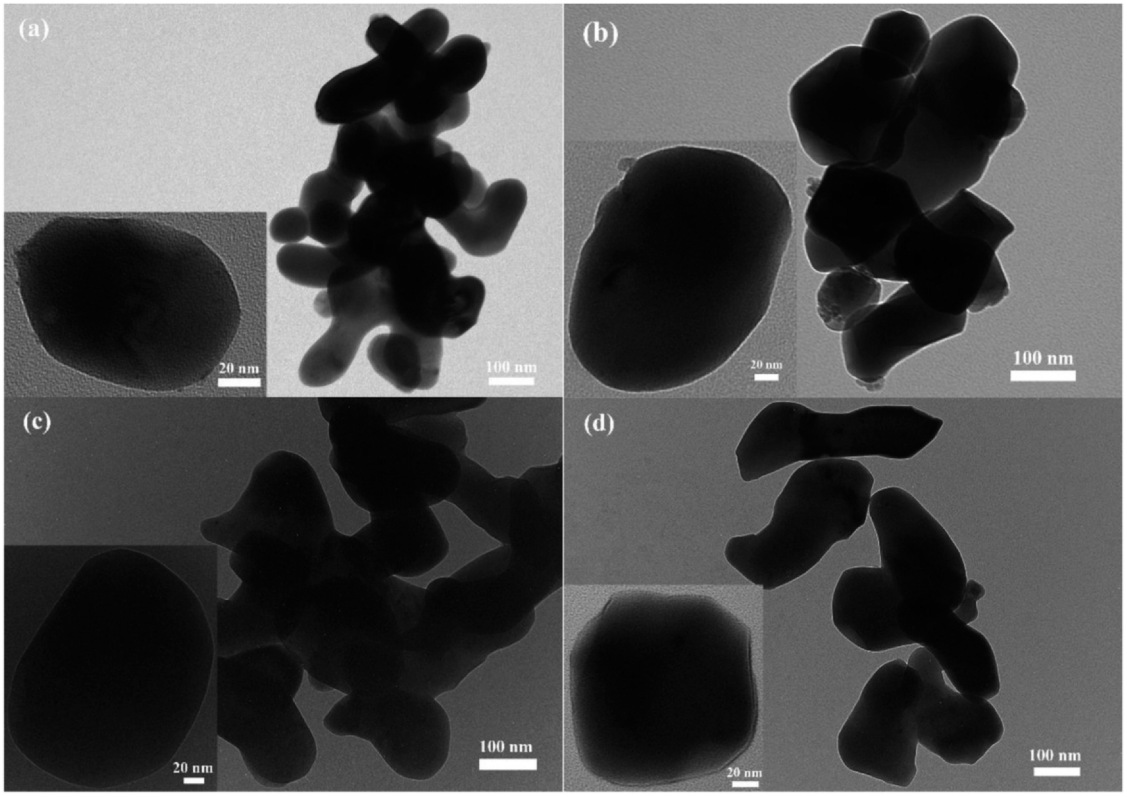

Fig. 5. Transmission electron microscopy (TEM) images of obtained $LiCoPO_4$, using 1: 6 (v/v) H_2O/DEG co-solvent, followed by firing at 600 °C in (a) Ar, (b) air, (c) 5% H_2/N_2 and (d) NH_3. (Inset) magnified TEM images of single LiCoPO4 particle [62].

Consequently, the method was one of the most suitable direction to prepare olivine structured materials with crystals smaller than 200 nm. The porosity of the particles had an essential effect on the electrochemical performance, since the voids are filled with electrolyte that improved the diffusion of lithium ion and affected on kinetics [77,78]. The charge-discharge profile demonstrated 134.6 mAh g^{-1} at 0.5 C-rate at room temperature [64]. Some authors like Rabanal et al. employed a conventional solid-state reaction where particles with less than 100 nm were obtained [66]. Mechanical grinding without carbon additives tended to have large aggregates, while addition of 8% of carbon altered and disaggregated crystals into smaller crystallites leading to have a uniform distribution of particles. Fig. 6 compares the electrochemical performances of pure LCP and carbon coated LCP/C. The relationship graph of specific capacity and cycle number proved that the smaller particles with grinding and carbon coating performed superior compare to larger grain sized bare LCP at different C rates.

Furthermore, the synthesis of LCP by a co-precipitation method using a micro reactor could effectively produce nanosphere-like particles with an average size of about 200 nm without agglomeration [68]. Thus, the electrochemical characteristics of the resulting LCP sample were significantly improved by enhancing the conductivity of the electrode, which represents an initial discharge capacity of up to 164 mAh g^{-1} at 0.1 C and high rate performance (117 mAh g^{-1} at 5 C). Another way to synthesize LCP/C composites with spherical nanoporous structure was obtained by a simple spray pyrolysis method. Conry et al. observed that reduced particle size (~ 70 nm) and carbon-coated (2.4 wt%) microstructured LCP cathode provided a sufficient electronic and ionic conductivity [69]. Consequently, these parameters were the explanation for the exhibition of high reversible capacity of 123 mAh g^{-1} at 0.1 C. Devaraju et al. described the promising fast supercritical method to obtain LCP high voltage cathode material, where characteristics such as particle size, shape and dispersion can be manipulated [70]. In their work synthesized plate-like shaped particles of LCP demonstrated great electrochemical performance (130 mAh g^{-1} for the first cycle and 98 mAh g^{-1} for the 10th cycle at 0.1 C). Explanation of the improved electrochemical activity was because of material's lowest side thickness. Optimal conditions to influence the morphology to produce plate-like LCP cathode was introduction of oleylamine and heating at 400 °C for 4 min. The molar ratio of oleylamine and metal ions was set to 10: 1. Li et al. synthesized core-shell structured

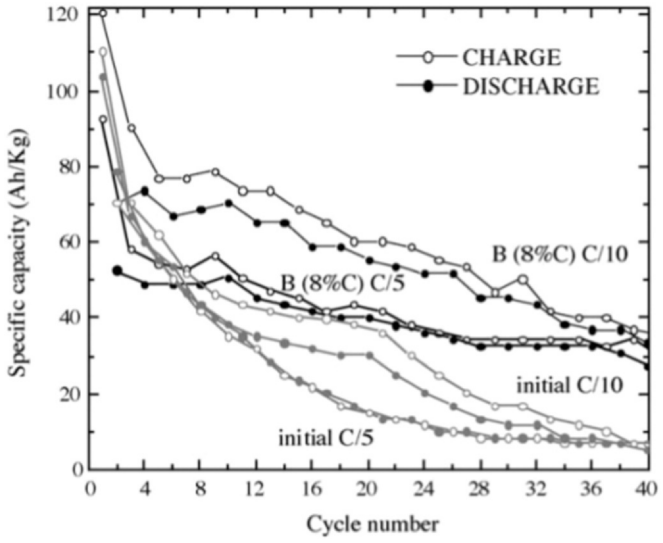

Fig. 6. Capacity of half cells vs. cycle number for bare LCP and LCP/8% C at cycling rates of C/5 and C/10 [66].

$LiCoPO_4$/C composite material by using a simple and rapid microwave heating process [25]. The surface of LCP particles was coated with carbon layer, while the carbon net was used as a connection part. Nanostructured morphology of cathode materials with an average particle size of approximately 150 nm in diameter positively influenced on electrochemical characteristics of lithium-ion batteries. Thus, cells with the nanosized LCP/C cathode exhibited excellent electrochemical performances (the initial discharge capacity 144 and 72.6 mAh g^{-1} for the 30th cycle at 0.1 C) and considered as an attractive approach. The particle size reduction of the LCP cathode obtained by various synthesizing methods with the electrochemical characteristics demonstrated in Table 2.

Regarding $LiNiPO_4$, similar techniques were utilized to synthesize nanostructured material. Identification of the relationship between reduced particle size of the cathode and electrochemical performance was observed. Zhang et al. explored a decisive factor of benzyl alcohol and glucose, which leads to the reduced particle size via combined solvothermal-solid-state reaction method [61]. The results proved that the water/benzyl alcohol mixture played a significant role in reducing the particle size and regulation the particle growth of LNP. Favorable effect of adding glucose as a carbon precursor during hydrothermal process is disaggregation of particles. So, LNP/C represented a high initial specific capacity of 143 mAh g^{-1} at 0.1 C. Interesting work was presented by Örnek et al. where a newly developed hard-template and solvothermal processes were used to obtain a core-shell structured nanoscale Co_3O_4 and CoO coated LNP [63]. It has been observed that surface-modified LNP/Co_3O_4 and LNP/CoO materials had smaller particle sizes than the bare LNP and it assisted in exhibiting high initial discharge capacity of 139 and 149 mAh g^{-1}, respectively. Moreover, these samples showed a stable voltage plateau at 5 V. In addition, they provided outstanding cycle life characteristics up to 80 charge-discharge cycles and a slight reduction in capacity at 0.1 C rate. Tao et al. observed the impact of citrate addition (as chelating agent) and annealing temperature on the electrochemical and physical properties of $LiNiPO_4$ using a sol-gel process [65]. The investigation established that particle size firstly grows by the annealing temperature rise, but it can be reduced by increasing the ratio of citrate/Li. Optimal conditions (700 °C and citrate/Li 2:1 by molar ratio) for obtaining spherical nanostructure of $LiNiPO_4$ with 100–200 nm particle sizes were explored to improve the reversible capacity of pure high-voltage $LiNiPO_4$ materials. As reported by Kumar et al., bare and carbon-coated $LiNiPO_4$ nanoparticles with an average size of 100 nm were produced via the polyvinylpyrrolidone (PVP) assisted polyol process that exhibited a voltage plateau at 5 V, corresponding to $Ni^{2+/3+}$ redox couple [79]. Bare and carbon-coated LNP nanoparticles show initial discharge capacities of 72 and 97 mAh g^{-1}, respectively. The high discharge capacity and cycling ability of carbon-coated LNP explained by nanosizing of particles, as well as the coating of carbon on the surface of particles, which contributes to improving the kinetic properties in lithium-ion batteries. Recently, Devaraju et al. published several research papers on regulating the size and morphology during synthesis of multiple cathodes, like phosphates, fluorophosphates, and silicates, using a supercritical fluid process and improving electrochemical characteristics related to size and shape [61,80–87]. The particles size reduction of the LNP cathode obtained by various synthesizing methods with the electrochemical characteristics depicted in Table 3.

Production of highly pure olivine cathodes can be done via many synthesis methods. One of the key parameters to enhance electrochemical performance is the preparation of smaller particles less than 100 nm with evenly distributed size, which can be achieved by proper design of fabrication route. From further observation it was clear that the crystal size could be reduced by surface coating of particles as well. It is striking to note that in accordance with the

Table 2
The electrochemical performance of $LiCoPO_4$ with reduced particle sizes synthesized via various methods.

Methods	Particle size	Electrochemical behavior			Ref.
		Initial discharge capacity, mAh g^{-1}	Current rate, C	Comments	
Solvothermal	500 nm	124	0.1	With a retention of 83% after 100 cycles	[60]
Hydrothermal	5–10 μm	107	0.5	The higher capacity after 20 cycles (47 mAh g^{-1}) can be achieved for 0.5 C.	[62]
Sol-gel	200 nm	134.6	0.5	The capacity retention was 59% for LCP.	[64]
Solid state	≤ 100 nm	40 Ah kg^{-1}	0.2	The specific capacity increased within cycling.	[66]
Co-precipitation	200 nm	164 117	0.1 5	Sample shows only 70% Columbic efficiency in the initial cycles.	[68]
Combination of spray pyrolysis and wet ball-milling	~ 87 nm	142 and 109	0.05 0.05	40 cycles corresponded to 87% of initial one at 0.1 C rate.	[72]
Spray pyrolysis	70 nm	123	0.1	Material exhibited a capacity retention of 95% over 20 cycles.	[69]
Supercritical fluid process	50–200 × 100–300 × 5–15 nm	130	0.1	98 mAh g^{-1} for the 10th cycle.	[70]
Microwave heating	~ 150 nm	93.3 (LCP) 144 (LCP/C)	0.1	LCP/C – 72.6 mAh g^{-1}, LCP_9.4 mAh g^{-1} after 30 cycles	[25]
Sol-gel assisted carbothermal synthesis	40 nm	Not given	Not given	Oxidation and reduction peaks were at 4.89 and 4.51 V	[73]

considered methods, the sol-gel process gives the most promising results in terms of electrochemical behavior due to the nanoscale particle size of material and phase purity. Although organics assisted procedures enable to obtain nano particles, the electrochemical performance did not show desirable results. At the same time the solid-state method benefits from easy preparation of ordered crystal structure, but it usually demands a higher synthesis temperature and a longer processing time, and results in an increase in particle size. Generally, agglomerated crystals negatively influence on electrochemical activity. In contrast, solution-based methods provide high purity, uniform size distribution, and small particle size; however, results suggested that performance was not close as in sol-gel method. The major disadvantages of these methods are complicated chemistry and multiple step routes. Although recent reports demonstrated that combined synthesis such as mechanical assisted particle synthesis could be the solution for large-scale production with controlled particle morphology, including the size and shape [88].

3. Surface modification

Generally, surface modification is applied to improve the electronic conductivity of various electrode materials. Particle surface is coated with contrasting electron-conductive matters such as metals [89] polymers [49,90], carbon (C) [55,91], and also composites [92,93]. Metal coating onto electrode surface is not widely applied technique and related reports are limited. Additionally, due to uneven distribution onto particle surfaces, and high level of reactivity with oxygen that form electron insulating layers, consumption of metals is not desirable. Another drawback of metal coating is that they are expensive for large scale applications, and difficult to control deposition process in manufacturing level. Worth to mention that more recent works also tried using electron conductive polymers to improve the electronic conductivity of cathode materials. Conductive polymers such as cyclized polyacrylonitrile (PAN), polypyrrole, and poly(3,4-ehtylenedioxythiophene) (known as PEDOT) also attracted attention because of their high electron conducting ability [90,94]. However, these polymers have diminished mechanical stability [95]. Thus, the simplicity of the carbon and obtaining process of the electron conductive layer without complex reaction mechanisms enables carbon to be an excellent choice for improvement of electrode's electronic conductivity. Another dominance of carbon as coating material was explained by a formation of Me_3P electron conductive phase during the heating in inert atmosphere [96,97]. As mentioned above the carbon coating also aids in reduction of a particle size, and elimination of particle agglomeration and growth [60,98,99]. While enhancing an ability to conduct electrons, the lithium ion conductivity also should be considered, as very thick layer of carbon may reduce the lithium ions transfer [100,101]. Thus, coating layer of carbon should be designed to be thin, uniform, and unbroken. The amount of carbon in cathode material varies from 0.5 and 2 wt% [102].

Generally, carbon coating on cathodes undergoes by several steps. First, LMP is synthesized, and then carbon sources such as citric acid, glucose, sucrose and, etc. are added with further heat treatment process. Moreover, there is also in-situ carbonization of olivine structures via several methods reported [25,69,103,104]. Choice of organics for carbon sources is crucial, as hydrogen may reduce transition metals and form additional D-element compound impurities [56,69,98,105,106]. Worth to note that carbon sources should interact with cathodes at lower temperatures. So the interaction and adhesion between active material and carbon should be higher by temperature incline [107–111].

3.1. $LiCoPO_4$/C

Reports by Wolfenstine et al. [112] and Gangulibabu et al. [113] suggested that carbon coating not only improved the electrical conductivity of LCP, but additionally assisted in forming the secondary phase like Co_2P that improves and enhances the electron conductivity further, and the formation of the phase occurs during heat treatment of carbon and LCP particles under inert environment. Wu et al. analyzed the effect of different carbon coating strategies on LCP and observed electrochemical performances of bare LCP, ex-situ and in-situ carbon coated LCPs [37]. Majority of reported works consume citric acid as the carbon source. The research reported that in-situ method of carbon coating outperformed other samples, as carbon layer was continuously uniform and complete on the surface of particles, as illustrated below in Fig. 7a. Ex-situ carbon layer had a thickness of around ~ 20 nm, while in-situ had ~ 2 nm. The initial discharge capacities of carbon-free LCP, ex-situ and in-situ LCP/C were 83.3, 104.2 and 120.3 mAh g^{-1} [37], respectively demonstrating that a very thin layer of carbon with uniform and complete coverage ensured higher conductivity of ions and electrons resulting in the better performance. Hou et al. investigated highly [010]-oriented self-assembled LCP/C nanoflakes as high-performance cathode for LIB [114]. Obtained in-situ LCP/C had a uniform carbon layer with a thickness of around 2 nm. The thin layer and ~ 1.5 wt% of carbon coated nanoflakes enhance the conductivity of the material. Results demonstrated that the initial discharge capacity of LCP/C

Table 3
The electrochemical performance of $LiNiPO_4$ with reduced particle sizes synthesized via various methods.

Methods	Particle size	Electrochemical performance		Comment	Ref.
		Initial discharge capacity, mAh g^{-1}	Current rate, C		
Solvothermal and solid state	LNP: ~ 2 µm LNP/C: 100–200 nm	83 (LNP) 143 (LNP/C)	0.1	The capacity of LNP/C is 72% larger than that of LNP at 0.1 C.	[61]
Hard-template silica & Hydrothermal	< 1 µm	149 (LNP/CoO)	0.1	It shows almost 82% capacity retention after 80 charge-discharge cycles.	[63]
Sol-gel	100–200 nm	Not given	Not given	The small particles provided shorter diffusion length and enhanced the lithium-ion transport.	[65]
Solid state	> 50 µm	Not given	Not given	The capacity reaches a stable value of ~ 50 mAh g^{-1} after 5 cycles, losing 10% of its initial value, and then it is retained for multiple cycles.	[67]
Polyol	~ 100 nm	72 (LNP) 97 (LNP/C)	0.1	It indicates that the carbon-coated LNP nanoparticles exhibited 25.8% higher discharge capacity as compared to bare LNP.	[79]
Supercritical fluid process	The rod-like LNP – from 100 to 200 nm in length, 50–80 nm in diameter. The plate like LNP – from 250 to 400 nm in length, 300–600 nm in width, and side thickness of less than 20 nm.	Not given	Not given	The Rietveld refinement analysis showed approximately 10% of antisite defects.	[71]

as a half-cell was 142.2 mAh g^{-1} at 0.1 C. A full cell was also assembled with $Li_4Ti_5O_{12}$ (LTO) as an anode, and the discharge capacity of 154.6 mAh g^{-1} at 0.1 C was obtained. The stable performance was observed up to 100 cycles with 93.1% capacity retention.

Li and Taniguchi investigated electrochemical behavior of LCP with different types of carbon sources such as sucrose, ascorbic, tartaric, citric acids, and polyvinyl pyrrolidone (PVP) that were prepared as ex-situ [115]. The output of the research showed that PVP was the optimal choice as a carbon source. The cathode powder from spray pyrolysis was wet ball milled with PVP and heat treated to obtain carbon coated LCP. The discharge capacity of bare LCP was 73 mAh g^{-1} and it was improved up to 110 mAh g^{-1} with PVP because of conductive carbon layer formation onto particles, which reduced particle size as well. The authors also stated that the annealing temperature of LCP and amount of PVP were crucial. The sample that had 0.3 wt% of carbon and annealed at 700 °C outperformed, and the crystal sizes were the smallest with a value of 77 nm [115]. Another work that compared carbon sources for LCP was by Maeyoshi et al. [98]. In this research, as organic additives carboxymethylcellulose (CMC), glucose and ascorbic acid were used and compared with carbon-free LCP [98]. The carbon content was varied in a range of 0.9–3.1%. The results demonstrated that organic carbon source as CMC was uniformly coated on the surface of particles. The thickness of layer was confirmed via TEM and it was approximately 6 nm. (Fig. 7b). The illustration via authors depicted that carbon from ascorbic acid covered the particles with large gaps, while from glucose source particles had isolated carbon. A sufficiently uniform and complete coating was obtained with CMC. The initial discharge capacities of carbon-free LCP, LCP/ascorbic acid, LCP/glucose and LCP/ CMC were 108.5, 112.9, 107.9, and 135.0 mAh g^{-1}, respectively. Excellence in performance of the last one was explained with high electronic conductivity of CMC and ability to reduce particles (Fig. 8c).

The unusual work on double carbon coated LCP nanocomposite was presented by Yu et al. [116]. The authors investigated bare, single and double layer coated LCP samples. The single carbon layered samples were as following: LCP with 3 wt% AB (LCP/AB), 5 wt % phenol-formaldehyde resins (LCP/PAS) and 10 wt% glucose (LCP/C). The double layer coating procedure was as follows: a) the first carbon layer was obtained with 10 wt% glucose beforehand; b) the second layer was produced by LCP with 1 wt% AB (LCP/C_AB) and 3 wt% PAS (LCP/C_PAS). The electrochemical performance of single carbon layered samples depicted the discharge capacities of 120.92, 121.07, and 138.06 mAh g^{-1} for LCP/C, LCP/PAS, and LCP/AB, respectively. The LCP/AB presented the highest capacity, however, it progressively decreased and after 30th cycle, it declined to 21.9 mAh g^{-1}. LCP/C and LCP/PAS kept their capacity up to 30 cycles. These values were described by the uniformity of carbon coating. Carbon layer from glucose and PAS was more homogenous and evenly distributed. In the case of the double layered samples, two layers of carbon reduced the particles down to 150 nm (particles of single layered carbon coating was 200 nm in size). The thickness of the inner and outer layers was different (Fig. 7c). TEM results exhibited that thickness of LCP/C_PAS sample's initial layer was 1.59 nm, and the outer had a value of 1 nm. LCP/C_AB showed 2 nm of a thick inner layer, and 2.41 nm of outer layer. The capacity delivery of LCP/C_PAS and LCP/C_AB 143.51 and 147.12 mAh g^{-1} at 0.1 C rate, respectively. The capacity retention of LCP/C_PAS and LCP/C_AB was 21.6% and 11.9% after 50 cycles (Fig. 8a, b).

3.2. $LiNiPO_4$/C

Depending on a choice of the fabrication method and organic additives as a carbon source, LNP with different shapes can be fabricated, such as nanorods and nanoplates [28]. Due to simplicity, ex-situ carbon coating technique was applied in the most of

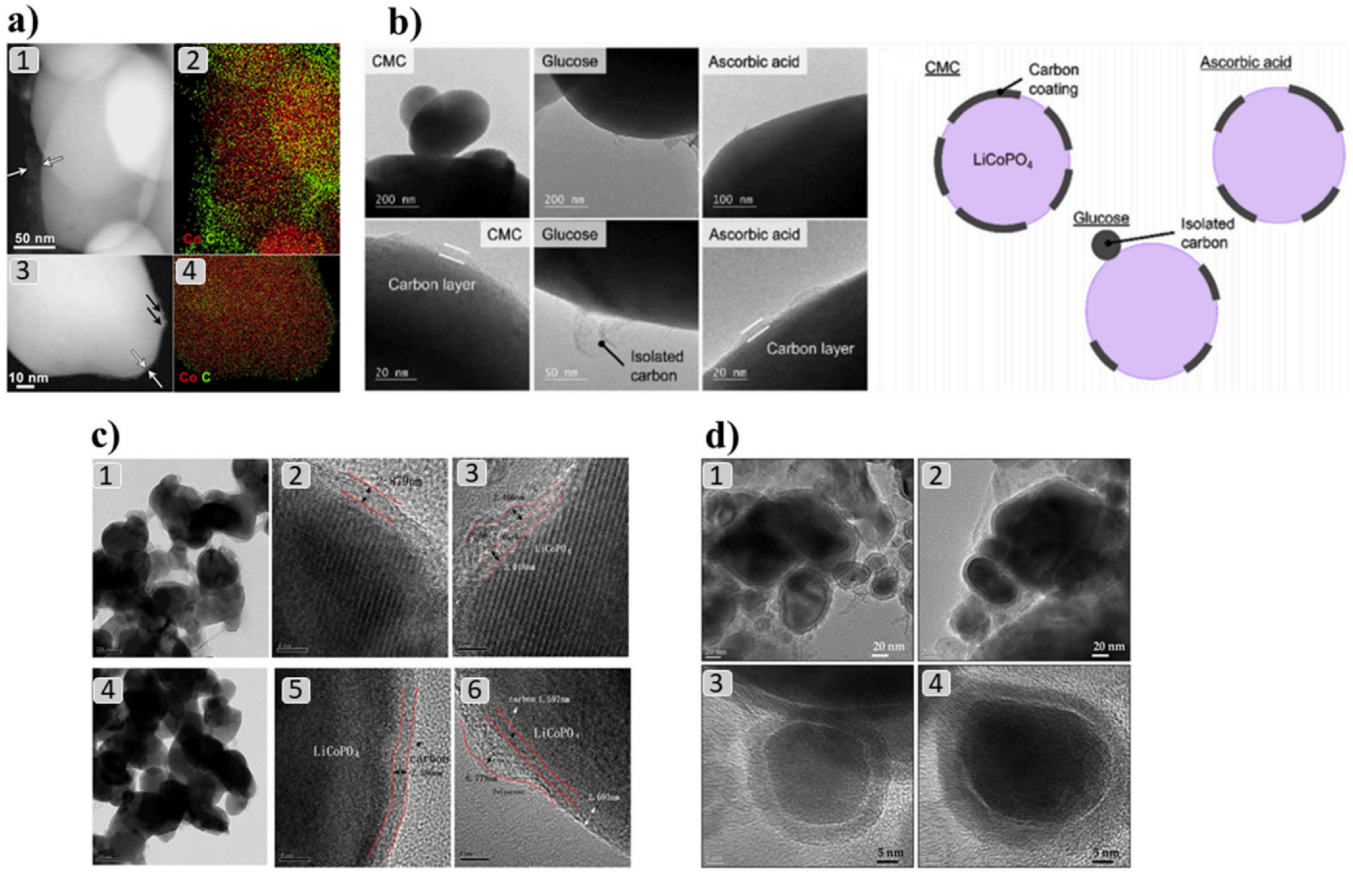

Fig. 7. HAADF-STEM of LCP/C ex-situ nanoparticles (1) with corresponding EDX (2), and LCP/C in-situ nanoparticle (3) with corresponding EDX map (4). White arrows point to the carbon coating (a) [37]; Carbon coated LCP particles by organics such as CMC, glucose, and ascorbic acid via TEM, and illustration of layer distribution onto LCP particles (b) [98]; TEM images of LCP/C_AB (1,2,3) and LCP/C_PAS (4,5,6) (c) [116]; TEM images of carbon (alginic acid) coated $LiNiPO_4$ (d) [117].

experimental works. Several authors consumed oxalic and acrylic acids as carbon sources for LNP and the discharge capacity of around 98 mAh g^{-1} was achieved [106]. Dimesso et al. investigated the influence of graphitic carbon foams on LNP [118]. The graphitic foam was coated on the surface of particles via in-situ technique. The specific capacity of LNP/C was 86 mAh g^{-1}. LNP was further modified by manipulating Ni content ($LiNi_yPO_4$ (y = 0.8–1.0)). As a result, uniformity of the coating depends on a value of y, as y = 1.0 had a uniform layer, while y < 1.0 had small cracks and voids. Electrochemical outputs depicted the discharge capacities of 76 and 122 mAh g^{-1} for $LiNi_{0.9}PO_4$/C and $LiNi_{0.8}PO_4$/C at 0.1 C, respectively. However, LNP/C and $LN_{0.9}P$ were stable up to 10 cycles with 10% of capacity fading, however, $LN_{0.8}P$ had the capacity fade of 86% after 10 cycles. These poor electrochemical behaviors were explained by a formation of instable delithiated crystalline phase of $Li_2Ni_3(P_2O_7)_2$ due to a not uniform carbon coating on particle surface.

However, some authors achieved higher capacity and longer cycle life by manipulating the organic solvents to assist in formation of cathode materials. Ornek et al. demonstrated a novel and effective low-level and longtime microwave and solvothermal (LLLTMSS) synthesis method for producing core-shell LNP/C [117]. As a carbon source alginic acid was used, which formed the most stable and uniform layer of carbon with a thickness of 4–5 nm (Fig. 7d). The synthesized LNP had an excellent discharge capacity of 150.2 mAh g^{-1}, while carbon-free LNP showed around 80 mAh g^{-1} at 0.1 C. LNP/C performed up to 100 cycles, by losing only 8% of capacity after 100 cycles. The later work of the same group demonstrated the importance of the reaction assisting solvents for carbon coating mechanism of LNP particles [119]. The work noted that organic precursors must intensively interact with LNP at lower temperatures in order to gain a high rate of adhesion at the starting point of the fabrication method. At a temperature of around 200–250 °C particles shatter and adheres onto the surface of active material, and by increasing the temperature particles uniformly distribute over the surface by forming a layer of carbon (Figs. 7d and 8d-f). The research *included influence* of different reaction media such as EG, isopropanol (IPA), isobutanol, and water on the properties of LNP/C material that previously reported. Among all solvents, LNP/C with IPA solvent medium depicted the highest discharge capacity of 157 mAh g^{-1} at 0.1 C rate. The material lost 19% of capacity after 80 cycles. Carbon coating on the surface of LNP was in a range of 5–6 nm. Similar research was conducted by Zhang et al. [61]. Glucose was used as a carbon source, and solvents such as benzyl alcohol and DI water were consumed as reaction assisting reagents. As a consequence, particles were 200 nm in size with initial capacities of 143, 91 and 45 mAh g^{-1} for 0.1 and 1 C.

Overall, carbon coating has a significant impact on the performance of high voltage olivine cathodes. The positive effects such as increased electronic conductivity and decreased particle size were achieved by a thin layer carbon coating. Particularly, coating by in-situ techniques demonstrated outstanding electrochemical performance where the discharge capacity close to the theoretical value could be achieved. In addition, carbon coating demonstrated compelling results as it helped to decline particle size. Careful observations demonstrated that the thickness of the carbon layer should be less than 6 nm, which enabled high electronic conductivity and sufficient lithium ion conduction, while thick layers inhibited the lithium ion motion.

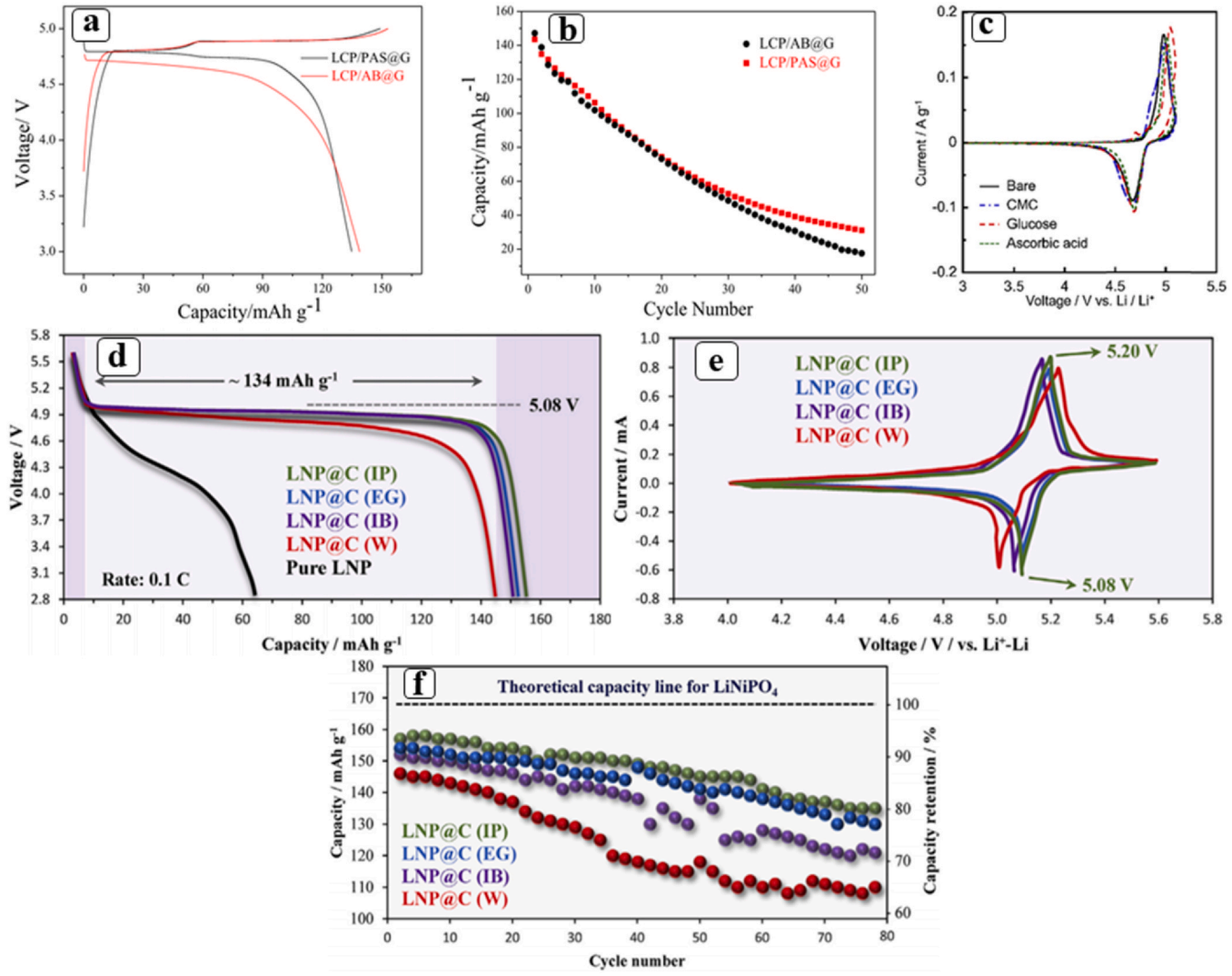

Fig. 8. Improvement of LCP and LNP by carbon coating. Charge and discharge curves (a) and cycle performances (b) of double carbon coated LCP composite; at 0.1 C [116]. CV profile of LCP with different carbon coatings (c) [98]. Charge and discharge curves (d), CV profile (e) and Cycling stability profiles of LNP by different solvents (f) [119].

4. Doping

The doping is a widely applied technique in crystallography to improve the performance of material by creating defects. The electronic conductivity, stability of materials, and electrochemical performance could be advanced via dopants. Another aspect of substitution is to reduce or increase a lattice size. The crystal structure of LCP and LNP were successfully doped with various cations such as Mg^{2+}, Sr^{2+}, V^{5+}, Y^{3+}, Cr^{3+}, Si^{4+} and Cu^{+} [111,117–138].

Work introduced by Kosova et al. on vanadium doped LCP concentrated on approaches to address the cyclability issue of (1-y) $LiCoPO_4$*y$Li_3V_2(PO_4)_3$, ($0 \leq y \leq 1$) [125]. A negligible amount of vanadium ions was incorporated into the LCP structure, while the rest of vanadium formed $Li_3V_2(PO_4)_3$. Result of the research indicated that low amount of vanadium (0.95 LCP – 0.05 $Li_3V_2(PO_4)_3$) enhanced electrochemical performance of the material compared to bare LCP due to the formation of sufficient amount of defects within the structure, which led to higher ionic and electronic conductivity of the material. In addition, the presence of $Li_3V_2(PO_4)_3$ monoclinic phase promoted lithium ion conduction. The final composition was 0.95 LCP/0.05 LVP, and it had an initial capacity of 101 mAh g^{-1}, and after 15 cycles it dropped to 95.5 mAh g^{-1}. F. Wang et al. highly promoted electrochemical performance of LCP cathode material by adding vanadium into the structure ($Li_{1+0.5x}Co_{1-x}V_x(PO_4)_{1+0.5x}$/C, (x = 0, 0.05, 0.10)) [136]. The electrochemical measurements showed that the addition of V^{5+} into LCP significantly improves the material's performance. Among all samples, cathode with formula of $Li_{1.025}Co_{0.95}V_{0.05}(PO_4)_{1.025}$ with carbon coating had the highest initial discharge capacity of 134.8 mAh g^{-1} at 0.1 C, while it was compared with LCP/C pristine structure which had a capacity of 112.2 mAh g^{-1} at 0.1 C. V^{5+} dopant also improved the cyclability of the material, and sample had 85% capacity retention after 25 cycles, while non-doped had 62%. The recent publication on vanadium-substituted LCP core for high voltage Li-ion batteries was also presented by K. Kreder et al. [135]. The work demonstrated the composition of $LiCo_{1-3x/2}V_{x/2}PO_4$ (LCVP), ($0.0 \leq x \leq 0.04$) that coated with various amounts of LFP. The initial discharge capacity of a sample with x = 0.02 ($LiCo_{0.97}V_{0.01}PO_4$) and 5% LFP coating was the highest among other samples, with a value of around 145 mAh g^{-1}. Only 51% capacity remained after 20 cycles. Moreover, the authors claimed that instability and decomposition of electrolyte at higher potential could also affect the further cyclability of electrodes. A work presented by A. Rajalashmi et al. also concentrated on properties of V^{5+} cation in LCP, $LiCo_{1-x}V_xPO_4$ and it was compared with undoped LCP [122]. The experiment basically based on electrochemical impedance spectroscopy (EIS) studies of modified materials. Results concluded

that V^{5+} cation did not make any remarkable improvement in the electrochemical behavior of LCP material.

Another element that was widely utilized and investigated as a dopant in high voltage olivine cathodes was iron. Improved cycle life of Fe-substituted LCP was presented by J. Allen et al., where 100% of discharge capacity (~ 105 mAh g^{-1}) was retained during 10 cycles, and 80% for 500 cycles [121]. The reason behind enhanced cyclability was explained via Fe^{3+} dopant. Doped cations occupied Li and Co sites simultaneously, which was proved by Rietveld refinement of XRD diffraction data, infrared spectroscopy, X-ray photoelectron spectroscopy and Mossbauer spectroscopy. A large occupation number of iron cations occurred in Co sites. The composition of this substitution was $Li_{0.92}Co_{0.8}Fe^{2+}_{0.12}Fe^{3+}_{0.08}PO_4$. The most recent research of the same author based on improvement of $LiCo_{0.9}Fe_{0.1}PO_4$ cathode with Cr and Si substitutions to examine full and half Li-ion cell performances [130]. J. Allen stated that initial Fe substituted LCP greatly improved the cycle life as well as it increased the energy density of the material. Moreover, modifications of $LiCo_{0.9}Fe_{0.1}PO_4$ with Cr ($LiCo_{0.829}Fe_{0.0976}Cr_{0.0488}PO_4$) and dopant led to owing further rise in the energy density, cycle life and rate capability, and reduction of reactivity of electrolyte with cathode by Si dopant ($LiCo_{0.820}Fe_{0.0976}Cr_{0.0488}Si_{0.00976}PO_4$) [130]. As a result, assembled half-cell with Cr, Si doped $LiCo_{0.9}Fe_{0.1}PO_4$ had the discharge capacity of 140 mAh g^{-1} at C/3 rate and no capacity fading over 250 cycles. A full cell with graphite was also assembled, and the initial capacity was at 135 mAh g^{-1} for 250 cycles and after it declined to 100 mAh g^{-1}. D. Lecce and et al. also put many efforts on development of high voltage cathodes by adding iron cation [138]. Earlier work of the authors demonstrated the optimization of Fe doped LCP, and it had a reversible capacity of 120 mAh g^{-1} at 0.1 C, and capacity retention of 78% remained during 20 cycles. The next investigation of the same author was the combination of two olivine cathodes such as $LiMnPO_4$ (LMP) and $LiCoPO_4$ [128]. By doing so they tried to solve problems of both cathodes like insulating nature of LMP and capacity fading of LCP. Furthermore, a modification of the combination occurred by adding metal cation as iron (Fe). The addition of the iron cation into the lattice was to enhance the electronic and ionic conductivity of LMP and reduce Jahn-Teller deformation. As a result, a final cathode material was $LiFe_{0.25}Mn_{0.5}Co_{0.25}PO_4$ and it had reversible capacities of around 105, 85 and 75 mAh g^{-1} at C/5, C/3 and 1 C rates with over 50 cycles with carbon coating. The latest study of D. Lecce et al. intensively tried to improve the performance of LCP with Mn and Fe [131]. Observation from the work showed that by increasing iron amount in LCP embellish electrodes reactivity, while the materials containing Mn ($LiCo_{1-x}Mn_xPO_4$) had poor behavior with diminished activity around 4.1 V vs. Li^+/Li [131]. Advanced research for these phenomena explanation was conducted and a detailed electrochemical impedance technique was applied. As a consequence, the examination revealed that substitution with manganese had a negative effect on LCP. The destitute function of the material was due to a charge transfer resistance growth. However, Fe doped LCP with a formula of $LiCo_{0.6}Fe_{0.4}PO_4$ and carbon coating depicted an operating plateau around 4.8 V with a capacity of 120 mAh g^{-1} and 80% of capacity remained after 20 cycles. S. Brutti et al. studied an interplay between local structure and transport properties in iron doped LCP olivine [120]. The author considered a partial substitution of Co ions in the olivine crystal with Fe^{2+} and Fe^{3+} to alter the concentration of anti-site defects, the natural concentration of lithium vacancies and lithium ion mobilization channel. Consequently, dopants modulated the lithium transport properties in the lattice. The output of the research found the most optimal material, $Li_{0.94-w}(Fe_{0.1}Co_{0.9})_{1.03}PO_4$ (LCfP/Ar) with a reversible capacity of 110 mAh g^{-1}.

The concept of a high-performance olivine-based cathode of $LiFe_xNi_yCo_zPO_4$ was studied by G. Pagot et al. [137]. From all variance, a material with a larger Co content, $Li_{1.009}Fe_{0.383}Ni_{0.081}Co_{0.694}(PO_4)_{1.000}$ ($LFNCP_{061}$) had charge and discharge profile over 150 cycles with a stable and constant capacity of 125 mAh g^{-1} at 0.5 C. However, after 150 cycles there was capacity fading due to decomposition of electrolyte over 4.5 V. The results also showed that higher Co content could prevent the fading as well. Although, both materials are high voltage cathodes, compare to LCP the doping of LNP has not been under a progressive research. There were only several reports on the advancement of LNP via substituting with other metal ions.

In the most of works the performance of LNP was attempted to improve with cobalt (Co) and the approach was chosen to enhance the electrical conductivity of the cathode where Co cations go to Ni occupancy [142]. The final cathode with the formula of $LiNi_{0.5}Co_{0.5}PO_4$/C delivered the discharge capacities varying from 145 to 159 mAh g^{-1}. V. Babu et al. compared structural and dielectric properties of LNP and $LiNi_{0.5}Co_{0.5}PO_4$ cathode materials [140]. The main focus of the research was impedance spectroscopy to examine electric conductivity of materials, as well as activation energy. As a result, dopant such as Co enlarges the lattice size and provides space for lithium ion migration. Activation energy calculations of these samples were determined and values 0.6075 eV and 0.7334 eV were obtained. The electric conductivity of $LiNi_{0.5}Co_{0.5}PO_4$ was higher than LNP. S. Devi et al. investigated structural and electrochemical characterizations of nanostructured $LiNi_{1-x}Co_xPO_4$ (x = 0 and 0.5), and reported the specific capacities of 172.4 mAh g^{-1} for LNP and 173.2 mAh g^{-1} for $LiNi_{0.5}Co_{0.5}PO_4$ at 0.1 C [123]. The capacity retention was 80% for 15 cycles.

S. Kartchikprabhu et al. reported carbon-free $LiNiPO_4$ (LNP) cathode material with manganese (Mn) dopant [139]. $LiNi_{1-x}Mn_xPO_4$, where dopant amount (x) varied from 0.05 to 0.20 were prepared via polyol method. The research concluded that the best performing doped material was $LiNi_{0.9}Mn_{0.1}PO_4$ and it exhibited an initial discharge capacity of 94.2 mAh g^{-1} while LNP had 75.6 mAh g^{-1} at 0.25 C. The materials performed over 100 cycles with potential range of 2.8 and 5.6 V and with 62% capacity retention. Another work presented by the same author designed neodymium (Nd) doped LNP cathode [141]. The variation of Nd^{3+} cation amount (x) in $LiNi_{1-x}Nd_xPO_4$ material were between 0.01 and 0.09. Among all these samples, the better performance was seen from $LiNi_{0.93}Nd_{0.07}PO_4$ with a maximum specific capacity of 95.2 mAh g^{-1} at 0.1 C rate. 95% of capacity remained after 50 cycles. Q. Tan et al. examined electrical and structural characteristics of $LiNi_{1-x}(Co_{0.5}Mn_{0.5})_xPO_4$ ($0 \le x \le 1$), and reported that in order to increase conductivity of cathode materials nickel content should be 0.2 [133]. The work presented by P. Tadesse et al. concentrated on an effect of aluminum dopant on the structure, electrical and dielectric properties of $LiNi_{0.5}Co_{0.5}PO_4$ cathode material [126]. $LiNi_{0.5}Co_{0.5-x}Al_xPO_4$ (x = 0.0, 0.05, 0.1 and 0.15) materials were prepared and tested, however, $LiNi_{0.5}Co_{0.4}Al_{0.1}PO_4$ displayed higher capacity among all other samples with value of 46.1 mAh g^{-1} for 10 cycles. The initial capacity of the material decreased to 17.1% after 10 cycles, and remaining discharge capacity was at 38.2 mAh g^{-1} with working potential of 2.25 and 4.8 V. The overall electrochemical result summary of these doped samples is demonstrated in Table 4.

Comprehensive review showed that the electronic conductivity of doped LCP and LNP have no significant difference from carbon coated LCP and LNP. It should be noted that after doping LCP and LNP with different types of transition metals were coated by carbon as well, and it is not clear which of these approaches has more effect on the materials performance. In order to maintain high operating potentials of these cathodes, the amount of dopant should be strictly controlled. Summarizing all recent works, it is obvious that considerable number of researchers tried to improve LCP and LNP through iron doping, as LFP commercial cathode demonstrates excellent performance in terms of cycle ability and rate capability. Unfortunately, it can be concluded that there is still broad research needed.

Table 4
The overall data of doped cathode materials of LCP/LNP.

Molecular formula	Outperformed samples	Potential, V	Capacity mAh g^{-1}	C rate	Ref.
(1-y)$LiCoPO_4$*y$Li_3V_2(PO_4)_3$	0.95 LCP – 0.05 $Li_3V_2(PO_4)_3$		101	0.1	[125]
$Li_{1+0.5x}Co_{1-x}V_x(PO_4)_{1+0.5x}$/C (x = 0, 0.05, 0.10)	$Li_{1.025}Co_{0.95}V_{0.05}(PO_4)_{1.025}$/C	4.1	134.8	0.1	[136]
$LiCo_{1-3x/2}$ $V_{x/2}PO_4$ (LCVP) (0.0 ≤ x ≤ 0.04) + 5% LFP	$LiCo_{0.97}V_{0.01}PO_4$ + 5% LFP	4.93	145	0.1	[135]
Fe-substituted $LiCoPO_4$	$LiCo_{0.8}Fe_{0.2}PO_4$	4.8	105	0.1	[121]
Fe doped LCP/C	$LiCo_{0.6}Fe_{0.4}PO_4$/C	4.8	120	0.1	[131]
Cr, Si doped $LiCo_{0.9}Fe_{0.1}PO_4$	$LiCo_{0.820}Fe_{0.0976}Cr_{0.0488}Si_{0.00976}PO_4$		140	0.3	[130]
Iron doped LCP LCfP	$Li_{0.94-w}(Fe_{0.1}Co_{0.9})_{1.03}PO_4$	4.8 V	110		[120]
Fe doped $LiMnCoPO_4$	$LiFe_{0.25}Mn_{0.5}Co_{0.25}PO_4$	4.1	105	0.2	[128]
$LiFe_xNi_yCo_zPO_4$	$Li_{1.009}Fe_{0.383}Ni_{0.081}Co_{0.694}(PO_4)_{1.000}$	4.5	125	0.5	[137]
$LiNi_{1-x}Co_xPO_4$/C	$LiNi_{0.5}Co_{0.5}PO_4$/C		159	0.1	[142]
$LiNi_{1-x}Co_xPO_4$	$LiNi_{0.5}Co_{0.5}PO_4$/C		173.2	0.1	[123]
$LiNi_{1-x}Mn_xPO_4$	$LiNi_{0.9}Mn_{0.1}PO_4$		94.2	0.25	[139]
$LiNi_{1-x}Nd_xPO_4$	$LiNi_{0.93}Nd_{0.07}PO_4$		95.2	0.1	[141]
$LiNi_{0.5}Co_{0.5-x}Al_xPO_4$	$LiNi_{0.5}Co_{0.4}Al_{0.1}PO_4$	4.8	46.1	0.1	[126]

5. Quantum mechanical calculations

Progress in material science for energy storage systems faces significant challenges that require a fundamental understanding that only can be resolved by computational simulations. Addition to this, computational hardware and simulation techniques have been widely exploited and expanded the scope and capability of computational applications. In the case of energy storage systems, the computer simulations allow to study materials at electronic and atomic levels. For instance, it enables to explain thermodynamic stabilities of crystals during lithiation and delithiation processes and ionic migration direction, interface issue of cathodes that cannot be properly evaluated by experimental works and etc. [142–151].

Calculation of energy and structure of positive electrodes can be done via density functional theory (DFT) - the most widely used technique in the field of solid state inorganic materials. The DFT methods take into consideration several levels of approximation [147]. In most cases, properties are the total energy, structure, the band structure of a material. Although many properties can be calculated, only two properties such as structure and energy are widely applied for cathode materials, in particular, the voltage, capacity, and cycling stability [147]. Meng et al. reviewed many types of cathodes using the first principal method to calculate the structural components [145]. Olivine phosphates were among the simulated cathodes and measurements like the redox potentials, the ion mobility, the phase transformation mechanisms, stability of structure change were simulated [145]. Hoang et al. investigated a crystal defects of LFP olivine and characterized them by their formation energy, and reported about the native charged point defects, and these defects were stable at one charge state only [144]. The electron and ionic conductivity of olivine phosphates (LMP) depend on the growth of hole polaron and lithium vacancy numbers through actions that can shift Fermi level and synthesis processes [144]. Another author (Xu et al.) that investigated olivine structure suggested that manipulation of band-structure related to electronic structure depends on doping or substitution of transition metal [151]. Some dopants occupy lithium and oxygen sites which further developed the electronic conductivity of materials. The first principal investigation of Mn-doped LCP was carried out by Zhi-Ping et al. [152]. The output of results demonstrated that manganese dopant changes the lattice parameters by shrinking the cell and tolerating the excellent repeated cycle ability of the battery. The research by H. Gwon et al. on combined first-principle calculations and experimental study on multi-component olivine cathodes [143]. Results have demonstrated very important conclusion reporting that Fe^{3+}/Fe^{2+}, Mn^{3+}/Mn^{2+}, Co^{3+}/Co^{2+} redox couples electrochemically active below the 4.9 V. It indicated that $LiMn_{1/3}Fe_{1/3}Co_{1/3}PO_4$ had one phase reaction for all lithium compositions by the effect of the presence of multi-components [143]. By other words, a several-phase reaction was converted into a one-phase reaction for the well-ordered, non-nanocrystalline olivine phase at RT with several elements doping [143]. M. Alfaruqi et al. examined DFT on mixed transition metals in olivine materials for energy storage applications [142]. A material with a formula of $LiNi_{0.5}Mn_{0.5}PO_4$ was compared with $LiMnPO_4$. The calculation estimated that presence of nickel in olivine structure positively influenced the structure favoring lithium intercalation and enhancing electronic conductivity [142]. The lithiation potential of the materials increased up to 4.27 V enabling high energy density. Furthermore, the activation energy of lithium ions mobility was decreased by such modifications further improving performance of the cathode [142]. Many simulation works might be difficult to implement in real time experiments because of uncontrollability of some parameters such as occupancy of particular elements at certain sites and creation of sufficient amount of vacancies. Thus, idealized calculated parameters should put into practical experimental works until simulated theoretical values are reached. Depending on improvement methods there is still considerable amount of work should be conducted preferably by combining all development approaches to prepare high performance materials for future applications.

6. Applications and future perspectives

Lithium transition metal (Co, Ni) phosphates have been widely studied as potential candidates for cathode materials in high-voltage lithium-ion batteries because of their structure that provides full lithiation and delithiation during charge and discharge processes. Numerous attempts have been considered in order to advance the performance of perspective high voltage cathode materials such as LCP and LNP. Up-to-date, the specific capacity of materials reached only approximately 80% and below. Unfortunately, the discharge capacity of these two cathodes remains only up to 10 – 20 cycles at lower rates. Despite these issues, a great progress could lead to implementation of these cathodes into all-solid-state battery system for large scale applications (Fig. 9). High working potentials of 4.8 and 5.2 V and advantages of the olivine structure favor them as excellent candidates for operation in EV and HV (Fig. 9). For instance, Okumura et al. applied olivine structured LCP in all-solid-state LIBs by forming $LiCoPO_4$-LATP composite cathode via spark plasma sintering (SPS) technique and analyzed its electrochemical activity by CV [153]. A reversible charge-discharge capacity of LCP was derived by CV at a scan rate of 0.5 mV s^{-1} at 150 °C. Taking into consideration the success of this work, further steps can be taken towards using other solid electrolytes based on lithium ion conducting solid and gel polymers and inorganic ceramics. Further progress in high voltage olivine structured cathodes in combination with suitable solid polymers will be a breakthrough in energy storage systems enabling them to accommodate high energy in smaller cell packages.

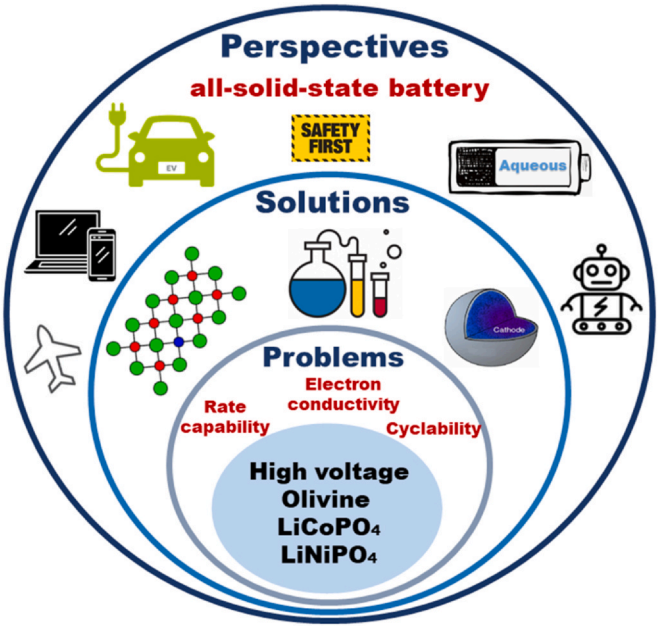

Fig. 9. Graphical illustration of problems, solutions and future perspectives of high potential cathodes.

Although progress in designing solid electrolytes has been admirable, liquid electrolytes are still widely consumed. Unfortunately, working potentials of these cathodes limit utilizing the commercial electrolyte that starts decomposing at 4.4 V. However, this process can be prevented by progressing additives for liquid electrolytes. Expanding this kind of work could contribute to utilization of high potential phosphate olivines.

Recently, the development of new types of energy storing that meets current demand has been gaining a significant attention. One of the latest interests is aqueous batteries that operates on lithium ion conduction mechanism [154]. Moreover, an experimental study where high potential electrode LCP utilized as a cathode in aqueous batteries was reported [155]. In the work tin (Sn) was used as an anode with aqueous electrolyte. A novel 1 V cell composed of Sn – LCP and lithium hydroxide aqueous solution had the reversible insertion and extraction of lithium ions and provided structural and cycling stability for over 25 cycles. Based on galvanostatic and cyclic voltammetric data after the fifth cycle, it was found that the Coulombic efficiency of the aqueous battery is close to 100%, providing a reversible discharge capacity of 80 mAh g^{-1} [155]. The same author reported olivine LNP for aqueous rechargeable battery [67]. During the oxidation process where Li-ions de-intercalated a side product as nickel (II) hydroxide (β-NiOOH) formed. As a result, lithium ions were not fully intercalated demonstrating a reversible performance for only couple of cycles. The highest discharge capacity of 55 mAh g^{-1} was obtained, and after 5 cycles it declined to 50 mAh g^{-1}. Evaluating the idea and progress of phosphate olivines in aqueous batteries open many opportunities for many research communities. Endeavors in this direction need to be continued to advance these cathodes for aqueous system that provides high safety with environmental friendliness.

The development of solid electrolytes such as polymer [156–159] and inorganic ceramic [160,161] enables assembling new generation high power cells with the high voltage cathodes towards lithium metal anode that could cycle with great stability. However, decade time dedicated research on the high voltage olivine structured cathode still struggles to maintain the current demand for implementation of the cathodes of $LiCoPO_4$ and $LiNiPO_4$ into the energy storage systems. In order to fully understand these cathodes weaknesses, detailed research from the computational side should be designed. Having the most required characteristics for the development of the next generation energy storage systems, these two cathodes ought to implement the theoretical calculations into real experimental works. By combining the output from several assumption and results, it can be properly concluded and found the future perspectives of these materials. Generally, the progress in the performance of these two high potential olivine cathodes not only advances all-solid-state battery field, but may also influence on environmentally friendly, non-hazardous aqueous energy storage systems. Overall, there were still improvements reported that can contribute to the progress in the field of all-solid-state and aqueous energy storage systems.

Declaration of Competing Interest

The authors declare that they have no known competing financial interests or personal relationships that could have appeared to influence the work reported in this paper.

Acknowledgment

This research was supported by the research grants #AP08855889 “Development of Flexible and Safe Next-Generation Li-Ion Batteries” and #AP09259764 “Engineering of Multifunctional Materials of Next Generation Batteries” from the Ministry of Education and Science of the Republic of Kazakhstan and #021220CRP0122 “Development of highly sensitive MOS based nano-film gas sensors” from Nazarbayev University.

References

[1] J.P. Pender, G. Jha, D.H. Youn, J.M. Ziegler, I. Andoni, E.J. Choi, A. Heller, B.S. Dunn, P.S. Weiss, R.M. Penner, C.B. Mullins, Electrode degradation in lithium-ion batteries, ACS Nano 14 (2020) 1243–1295, https://doi.org/10.1021/acsnano.9b04365
[2] A. Manthiram, A reflection on lithium-ion battery cathode chemistry, Nat. Commun. 11 (2020) 1–9, https://doi.org/10.1038/s41467-020-15355-0
[3] W. Lee, S. Muhammad, C. Sergey, H. Lee, J. Yoon, Y.M. Kang, W.S. Yoon, Advances in the cathode materials for lithium rechargeable batteries, Angew. Chem. Int. Ed. 59 (2020) 2578–2605, https://doi.org/10.1002/anie.201902359
[4] N. Baikalov, N. Serik, S. Kalybekkyzy, I. Kurmanbayeva, Z. Bakenov, A. Mentbayeva, High mass-loading sulfur-composite cathode for lithium-sulfur batteries, Front. Energy Res. 8 (2020) 1–8, https://doi.org/10.3389/fenrg.2020.00207
[5] A. Burukhin, Hydrothermal synthesis of $LiCoO_2$ for lithium rechargeable batteries, Solid State Ion. 151 (2002) 259–263, https://doi.org/10.1016/S0167-2738(02)00721-X
[6] O.A. Brylev, O.A. Shlyakhtin, T.L. Kulova, A.M. Skundin, Y.D. Tretyakov, Influence of chemical prehistory on the phase formation and electrochemical performance of $LiCoO_2$ materials, Solid State Ion. 156 (2003) 291–299, https://doi.org/10.1016/S0167-2738(02)00686-0
[7] M. Broussely, F. Perton, P. Biensan, J.M. Bodet, J. Labat, A. Lecerf, C. Delmas, A. Rougier, J.P. Pérès, Li_xNiO_2, a promising cathode for rechargeable lithium batteries, J. Power Sources 54 (1995) 109–114, https://doi.org/10.1016/0378-7753(94)02049-9
[8] Y.K. Sun, I.H. Oh, Synthesis of $LiNiO_2$ powders by a sol-gel method, J. Mater. Sci. Lett. 16 (1997) 30–32, https://doi.org/10.1023/A:1018532313681
[9] J. Cho, T.-J. Kim, B. Park, The effect of a metal-oxide coating on the cycling behavior at 55 °C in orthorhombic $LiMnO_2$ cathode materials, J. Electrochem. Soc. 149 (2002) A288, https://doi.org/10.1149/1.1446870
[10] S. Azam, S. Mehmood, L. Tabassam, A.S. Bhatti, Structural and electrochemical characteristics of o-$LiMnO_2$-MWCNTs nanocomposites, Phys. B Condens. Matter 575 (2019) 411695, https://doi.org/10.1016/j.physb.2019.411695
[11] S.T. Myung, F. Maglia, K.J. Park, C.S. Yoon, P. Lamp, S.J. Kim, Y.K. Sun, Nickel-rich layered cathode materials for automotive lithium-ion batteries: achievements and perspectives, ACS Energy Lett. 2 (2017) 196–223, https://doi.org/10.1021/acsenergylett.6b00594
[12] C. Song, W. Wang, H. Peng, Y. Wang, C. Zhao, H. Zhang, Q. Tang, J. Lv, X. Du, Y. Dou, Improving the electrochemical performance of $LiNi_{0.80}Co_{0.15}Al_{0.05}O_2$ in lithium ion batteries by $LiAlO_2$ surface modification, Appl. Sci. 8 (2018) 378, https://doi.org/10.3390/app8030378

[13] T. Ohzuku, Y. Makimura, Layered lithium insertion material of $LiCo_{1/3}Ni_{1/3}Mn_{1/3}O_2$ for lithium-ion batteries, Chem. Lett. 30 (2001) 642–643, https://doi.org/10.1246/cl.2001.642

[14] H.J. Noh, S. Youn, C.S. Yoon, Y.K. Sun, Comparison of the structural and electrochemical properties of layered $Li[Ni_xCo_yMn_z]O_2$ (x = 1/3, 0.5, 0.6, 0.7, 0.8 and 0.85) cathode material for lithium-ion batteries, J. Power Sources 233 (2013) 121–130, https://doi.org/10.1016/j.jpowsour.2013.01.063

[15] L. Hong, K. Yang, M. Tang, A mechanism of defect-enhanced phase transformation kinetics in lithium iron phosphate olivine, Npj Comput. Mater. 5 (2019) 1–9, https://doi.org/10.1038/s41524-019-0255-3

[16] K. Yang, M. Tang, Three-dimensional phase evolution and stress-induced non-uniform Li intercalation behavior in lithium iron phosphate, J. Mater. Chem. A 8 (2020) 3060–3070, https://doi.org/10.1039/c9ta11697d

[17] C.M. Julien, A. Mauger, K. Zaghib, H. Groult, Comparative issues of cathode materials for Li-ion batteries, Inorganics 2 (2014) 132–154, https://doi.org/10.3390/inorganics2010132

[18] A. Mesnier, A. Manthiram, Synthesis of $LiNiO_2$ at moderate oxygen pressure and long-term cyclability in lithium-ion full cells, ACS Appl. Mater. Interfaces 12 (2020) 52826–52835, https://doi.org/10.1021/acsami.0c16648

[19] L.H. Hu, F.Y. Wu, C. Te Lin, A.N. Khlobystov, L.J. Li, Graphene-modified $LiFePO_4$ cathode for lithium ion battery beyond theoretical capacity, Nat. Commun. 4 (2013) 1–7, https://doi.org/10.1038/ncomms2705

[20] Y. Fu, Q. Wei, G. Zhang, Y. Zhong, N. Moghimian, X. Tong, S. Sun, $LiFePO_4$ -graphene composites as high-performance cathodes for lithium-ion batteries: The impact of size and morphology of graphene, Materials Basel 16 (2019), https://doi.org/10.3390/ma12060842

[21] A. Maurel, S. Grugeon, B. Fleutot, M. Courty, K. Prashantha, H. Tortajada, M. Armand, S. Panier, L. Dupont, Three-dimensional printing of a $LiFePO_4$/graphite battery cell via fused deposition modeling, Sci. Rep. 9 (2019) 1–14, https://doi.org/10.1038/s41598-019-54518-y

[22] R. Sharabi, E. Markevich, V. Borgel, G. Salitra, D. Aurbach, G. Semrau, M.A. Schmidt, N. Schall, C. Stinner, Significantly improved cycling performance of $LiCoPO_4$ cathodes, Electrochem. Commun. 13 (2011) 800–802, https://doi.org/10.1016/j.elecom.2011.05.006

[23] N.N. Bramnik, K.G. Bramnik, T. Buhrmester, C. Baehtz, H. Ehrenberg, H. Fuess, Electrochemical and structural study of $LiCoPO_4$-based electrodes, J. Solid State Electrochem. 8 (2004) 558–564, https://doi.org/10.1007/s10008-004-0497-x

[24] B. Jin, H.B. Gu, K.W. Kim, Effect of different conductive additives on charge/discharge properties of $LiCoPO_4$/Li batteries, J. Solid State Electrochem. 12 (2008) 105–111, https://doi.org/10.1007/s10008-007-0367-4

[25] H.H. Li, J. Jin, J.P. Wei, Z. Zhou, J. Yan, Fast synthesis of core-shell $LiCoPO_4$/C nanocomposite via microwave heating and its electrochemical Li intercalation performances, Electrochem. Commun. 11 (2009) 95–98, https://doi.org/10.1016/j.elecom.2008.10.025

[26] K. Amine, H. Yasuda, M. Yamachi, Olivine $LiCoPO_4$ as 4.8 V electrode material for lithium batteries, Electrochem. Solid-State Lett. 3 (2000) 178–179, https://doi.org/10.1149/1.1390994

[27] L. Dimesso, D. Becker, C. Spanheimer, W. Jaegermann, Investigation of graphitic carbon foams/$LiNiPO_4$ composites, J. Solid State Electrochem. 16 (2012) 3791–3798, https://doi.org/10.1007/s10008-012-1817-1

[28] M. Kempaiah Devaraju, Q. Duc Truong, H. Hyodo, Y. Sasaki, I. Honma, Synthesis, characterization and observation of antisite defects in $LiNiPO_4$ nanomaterials, Sci. Rep. 5 (2015) 1–8, https://doi.org/10.1038/srep11041

[29] M. Prabu, S. Selvasekarapandian, A.R. Kulkarni, S. Karthikeyan, G. Hirankumar, C. Sanjeeviraja, Structural, dielectric, and conductivity studies of yttrium-doped $LiNiPO_4$ cathode materials, Ionics Kiel. 17 (2011) 201–207, https://doi.org/10.1007/s11581-011-0535-5

[30] M. Prabu, S. Selvasekarapandian, A.R. Kulkarni, S. Karthikeyan, C. Sanjeeviraja, Influence of europium doping on conductivity of $LiNiPO_4$, Trans. Nonferrous Met. Soc. China Engl. Ed. 22 (2012) 342–347, https://doi.org/10.1016/S1003-6326(11)61181-3

[31] S. Karthickprabhu, G. Hirankumar, A. Maheswaran, C. Sanjeeviraja, R.S. Daries Bella, Structural and conductivity studies on $LiNiPO_4$ synthesized by the polyol method, J. Alloy. Compd. 548 (2013) 65–69, https://doi.org/10.1016/j.jallcom.2012.08.141

[32] C.M. Julien, A. Mauger, K. Zaghib, R. Veillette, H. Groult, Structural and electronic properties of the $LiNiPO_4$ orthophosphate, Ionics Kiel. 18 (2012) 625–633, https://doi.org/10.1007/s11581-012-0671-6

[33] L. Vijayan, R. Cheruku, G. Govindaraj, Electrical, optical and magnetic investigations on $LiNiPO_4$ based olivines synthesized by solution combustion technique, Mater. Res. Bull. 50 (2014) 341–347, https://doi.org/10.1016/j.materresbull.2013.10.028

[34] A.M. Nolan, Y. Liu, Y. Mo, Solid-state chemistries stable with high-energy cathodes for lithium-ion batteries, ACS Energy Lett. 4 (2019) 2444–2451, https://doi.org/10.1021/acsenergylett.9b01703

[35] L. Wang, H. Zhang, Q. Liu, J. Wang, Y. Ren, X. Zhang, G. Yin, J. Wang, P. Zuo, Modifying high-voltage olivine-type $LiMnPO_4$ cathode via Mg substitution in high-orientation crystal, ACS Appl. Energy Mater. 1 (2018) 5928–5935, https://doi.org/10.1021/acsaem.8b00923

[36] A. Örnek, Positive effects of a particular type of microwave-assisted methodology on the electrochemical properties of olivine $LiMPO_4$ (M = Fe, Co and Ni) cathode materials, Chem. Eng. J. 331 (2018) 501–509, https://doi.org/10.1016/j.cej.2017.09.007

[37] X. Wu, F. Rohman, M. Meledina, H. Tempel, R. Schierholz, H. Kungl, J. Mayer, R.A. Eichel, Analysis of the effects of different carbon coating strategies on structure and electrochemical behavior of $LiCoPO_4$ material as a high-voltage cathode electrode for lithium ion batteries, Electrochim. Acta 279 (2018) 108–117, https://doi.org/10.1016/j.electacta.2018.05.067

[38] T. Nhat, P. Nguyen, C. Karuppiah, W. Chien, S. Wu, R. Jose, S.J. Lue, C. Yang, Mechanical alloy coating of LATP decorated porous carbon on $LiFe_{1/3}Mn_{1/3}Co_{1/3}PO_4$/C composite cathode for high-voltage Li-ion battery, Electrochim. Acta (2020) 136980, https://doi.org/10.1016/j.electacta.2020.136980

[39] H. Zhang, Y. Gong, J. Li, K. Du, Y. Cao, J. Li, Selecting substituent elements for $LiMnPO_4$ cathode materials combined with density functional theory (DFT) calculations and experiments, J. Alloy. Compd. 793 (2019) 360–368, https://doi.org/10.1016/j.jallcom.2019.04.191

[40] A. Yamada, M. Hosoya, S.C. Chung, Y. Kudo, K. Hinokuma, K.Y. Liu, Y. Nishi, Olivine-type cathodes: achievements and problems, J. Power Sources 119–121 (2003) 232–238, https://doi.org/10.1016/S0378-7753(03)00239-8

[41] M.F. Sgroi, R. Lazzaroni, D. Beljonne, D. Pullini, Doping $LiMnPO_4$ with cobalt and nickel: a first principle study, Batteries 3 (2017) 1–10, https://doi.org/10.3390/batteries3020011

[42] J.B. Goodenough, Cathode materials: a personal perspective, J. Power Sources 174 (2007) 996–1000, https://doi.org/10.1016/j.jpowsour.2007.06.217

[43] C. Fongy, A.-C. Gaillot, S. Jouanneau, D. Guyomard, B. Lestriez, Ionic vs electronic power limitations and analysis of the fraction of wired grains in $LiFePO_4$ composite electrodes, J. Electrochem. Soc. 157 (2010) A885, https://doi.org/10.1149/1.3432559

[44] K. Zaghib, A. Guerfi, P. Hovington, A. Vijh, M. Trudeau, A. Mauger, J.B. Goodenough, C.M. Julien, Review and analysis of nanostructured olivine-based lithium recheargeable batteries: status and trends, J. Power Sources 232 (2013) 357–369, https://doi.org/10.1016/j.jpowsour.2012.12.095

[45] A.K. Padhi, K.S. Nanjundaswamy, J.B. Goodenough, Phospho-olivines as positive-electrode materials for rechargeable lithium batteries, J. Electrochem. Soc. 144 (1997) 1188–1194, https://doi.org/10.1149/1.1837571

[46] M.G. Pamato, F. Nestola, D. Novella, J.R. Smyth, D. Pasqual, G.D. Gatta, M. Alvaro, L. Secco, The high-pressure structural evolution of olivine along the forsterite–fayalite join, Minerals 9 (2019) 1–11, https://doi.org/10.3390/min9120790

[47] J.D. Birle, G.V. Gibbs, P.B. Moore, J.V. Smith, Crystal structures of natural olivines, Am. Mineral. 53 (1968) 807–824 ⟨https://pubs.geoscienceworld.org/msa/ammin/article/53/5-6/807/542440/Crystal-structures-of-natural-olivines⟩.

[48] M.M. Doeff, J.D. Wilcox, R. Kostecki, G. Lau, Optimization of carbon coatings on $LiFePO_4$, J. Power Sources 163 (2006) 180–184, https://doi.org/10.1016/j.jpowsour.2005.11.075

[49] H.-C. Dinh, I.-H. Yeo, W. Il Cho, S. Mho, Characteristics of conducting polymer-coated nanosized $LiFePO_4$ cathode in the Li^+ batteries, ECS Trans. 28 (2019) 167–175, https://doi.org/10.1149/1.3490696

[50] S.L. Bewlay, K. Konstantinov, G.X. Wang, S.X. Dou, H.K. Liu, Conductivity improvements to spray-produced $LiFePO_4$ by addition of a carbon source, Mater. Lett. 58 (2004) 1788–1791, https://doi.org/10.1016/j.matlet.2003.11.008

[51] J. Li, W. Yao, S. Martin, D. Vaknin, Lithium ion conductivity in single crystal $LiFePO_4$, Solid State Ion. 179 (2008) 2016–2019, https://doi.org/10.1016/j.ssi.2008.06.028

[52] M. Safari, C. Delacourt, Modeling of a commercial graphite/$LiFePO_4$ cell, J. Electrochem. Soc. 158 (2011) A562, https://doi.org/10.1149/1.3567007

[53] Y. Hu, M.M. Doeff, R. Kostecki, R. Fiñones, Electrochemical performance of sol-gel synthesized $LiFePO_4$ in lithium batteries, J. Electrochem. Soc. 151 (2004) A1279, https://doi.org/10.1149/1.1768546

[54] V. Srinivasan, J. Newman, Existence of path-dependence in the $LiFePO_4$ electrode, Electrochem. Solid-State Lett. 9 (2006) A110, https://doi.org/10.1149/1.2159299

[55] C. Gong, Z. Xue, S. Wen, Y. Ye, X. Xie, Advanced carbon materials/olivine $LiFePO_4$ composites cathode for lithium ion batteries, J. Power Sources 318 (2016) 93–112, https://doi.org/10.1016/j.jpowsour.2016.04.008

[56] N. Laszczynski, A. Birrozzi, K. Maranski, M. Copley, M.E. Schuster, S. Passerini, Effect of coatings on the green electrode processing and cycling behaviour of $LiCoPO_4$, J. Mater. Chem. A 4 (2016) 17121–17128, https://doi.org/10.1039/c6ta05262b

[57] S.M. Oh, S.T. Myung, Y.K. Sun, Olivine $LiCoPO_4$-carbon composite showing high rechargeable capacity, J. Mater. Chem. 22 (2012) 14932–14937, https://doi.org/10.1039/c2jm31933k

[58] M. Zhang, N. Garcia-Araez, A.L. Hector, Understanding and development of olivine $LiCoPO_4$ cathode materials for lithium-ion batteries, J. Mater. Chem. A 6 (2018) 14483–14517, https://doi.org/10.1039/c8ta04063j

[59] A. Vadivel Murugan, T. Muraliganth, P.J. Ferreira, A. Manthiram, Dimensionally modulated, single-crystalline $LiMPO_4$ (M= Mn, Fe, Co, and Ni) with nano-thumblike shapes for high-power energy storage, Inorg. Chem. 48 (2009) 946–952, https://doi.org/10.1021/ic8015723

[60] B. Wu, H. Xu, D. Mu, L. Shi, B. Jiang, L. Gai, L. Wang, Q. Liu, L. Ben, F. Wu, Controlled solvothermal synthesis and electrochemical performance of $LiCoPO_4$ submicron single crystals as a cathode material for lithium ion batteries, J. Power Sources 304 (2016) 181–188, https://doi.org/10.1016/j.jpowsour.2015.11.023

[61] Y. Zhang, Y. Pan, J. Liu, G. Wang, D. Cao, Synthesis and electrochemical studies of carbon-modified $LiNiPO_4$ as the cathode material of Li-ion batteries, Chem. Res. Chin. Univ. 31 (2015) 117–122, https://doi.org/10.1007/s40242-015-4261-9

[62] C. Neef, H.P. Meyer, R. Klingeler, Morphology-controlled two-step synthesis and electrochemical studies on hierarchically structured $LiCoPO_4$, Solid State Sci. 48 (2015) 270–277, https://doi.org/10.1016/j.solidstatesciences.2015.08.021

[63] A. Örnek, The synthesis of novel $LiNiPO_4$ core and Co_3O_4/CoO shell materials by combining them with hard-template and solvothermal routes, J. Colloid Interface Sci. 504 (2017) 468–478, https://doi.org/10.1016/j.jcis.2017.05.118

[64] K. Kim, J.K. Kim, Comparison of structural characteristics and electrochemical properties of $LiMPO_4$ (M=Fe, Mn, and Co) olivine compounds, Mater. Lett. 176 (2016) 244–247, https://doi.org/10.1016/j.matlet.2016.04.145

[65] Y. Tao, D. Yi, B. Zhu, Synthesis of LiNiPO4 via citrate sol–gel route, J. Sol. Gel Sci. Technol. 87 (2018) 240–244, https://doi.org/10.1007/s10971-018-4690-2

[66] M.E. Rabanal, M.C. Gutierrez, F. Garcia-Alvarado, E.C. Gonzalo, M.E. Arroyo-de Dompablo, Improved electrode characteristics of olivine-$LiCoPO_4$ processed by high energy milling, J. Power Sources 160 (2006) 523–528, https://doi.org/10.1016/j.jpowsour.2005.12.071

[67] M. Minakshi, P. Singh, D. Appadoo, D.E. Martin, Synthesis and characterization of olivine $LiNiPO_4$ for aqueous rechargeable battery, Electrochim. Acta 56 (2011) 4356–4360, https://doi.org/10.1016/j.electacta.2011.01.017

[68] H. Zhao, Y. Yu, G. Wang, Y. Chen, X. Liu, H. Yang, Synthesis of nanosphere-like $LiCoPO_4$ with excellent electrochemical performance via micro reactor assisted co-precipitation method, Funct. Mater. Lett. 11 (2018) 1850037, https://doi.org/10.1142/S1793604718500376

[69] J. Liu, T.E. Conry, X. Song, L. Yang, M.M. Doeff, T.J. Richardson, Spherical nanoporous $LiCoPO_4$/C composites as high performance cathode materials for rechargeable lithium-ion batteries, J. Mater. Chem. 21 (2011) 9984–9987, https://doi.org/10.1039/c1jm10793c

[70] M.K. Devaraju, D. Rangappa, I. Honma, Controlled synthesis of plate-like $LiCoPO_4$ nanoparticles via supercritical method and their electrode property, Electrochim. Acta 85 (2012) 548–553, https://doi.org/10.1016/j.electacta.2012.08.108

[71] M. Kempaiah Devaraju, Q. Duc Truong, H. Hyodo, Y. Sasaki, I. Honma, Synthesis, characterization and observation of antisite defects in $LiNiPO_4$ nanomaterials, Sci. Rep. 5 (2015) 1–8, https://doi.org/10.1038/srep11041

[72] T.N.L. Doan, I. Taniguchi, Preparation of LiCoPO4/C nanocomposite cathode of lithium batteries with high rate performance, J. Power Sources 196 (2011) 5679–5684, https://doi.org/10.1016/j.jpowsour.2011.02.039

[73] P.N. Poovizhi, S. Selladurai, Study of pristine and carbon-coated $LiCoPO_4$ olivine material synthesized by modified sol-gel method, Ionics Kiel. 17 (2011) 13–19, https://doi.org/10.1007/s11581-010-0496-0

[74] Y. Hong, Z. Tang, S. Wang, W. Quan, Z. Zhang, High-performance $LiMnPO_4$ nanorods synthesized via a facile EG-assisted solvothermal approach, J. Mater. Chem. A 3 (2015) 10267–10274, https://doi.org/10.1039/c5ta01218j

[75] X. Qin, J. Wang, J. Xie, F. Li, L. Wen, X. Wang, Hydrothermally synthesized $LiFePO_4$ crystals with enhanced electrochemical properties: Simultaneous suppression of crystal growth along [010] and antisite defect formation, Phys. Chem. Chem. Phys. 14 (2012) 2669–2677, https://doi.org/10.1039/c2cp23433e

[76] J. Ludwig, D. Haering, M.M. Doeff, T. Nilges, Particle size-controllable microwave-assisted solvothermal synthesis of the high-voltage cathode material $LiCoPO_4$ using water/ethylene glycol solvent blends, Solid State Sci. 65 (2017) 100–109, https://doi.org/10.1016/j.solidstatesciences.2017.01.009

[77] R. Dominko, M. Bele, M. Gaberscek, M. Remskar, D. Hanzel, J.M. Goupil, S. Pejovnik, J. Jamnik, Porous olivine composites synthesized by sol-gel technique, J. Power Sources 153 (2006) 274–280, https://doi.org/10.1016/j.jpowsour.2005.05.033

[78] S. Ju, T. Liu, H. Peng, G. Li, K. Chen, A facile synthesis route for porous spherical $LiFePO_4$/C microscale secondary particles, Mater. Lett. 93 (2013) 194–198, https://doi.org/10.1016/j.matlet.2012.11.083

[79] P.R. Kumar, V. Madhusudhan Rao, B. Nageswararao, M. Venkateswarlu, N. Satyanarayana, Enhanced electrochemical performance of carbon-coated $LiMPO_4$ (M = Co and Ni) nanoparticles as cathodes for high-voltage lithium-ion battery, J. Solid State Electrochem 20 (2016) 1855–1863, https://doi.org/10.1007/s10008-016-3151-5

[80] M.K. Devaraju, Q.D. Truong, I. Honma, Synthesis of Li_2CoSiO_4 nanoparticles and structure observation by annular bright and dark field electron microscopy, RSC Adv. 3 (2013) 20633–20638, https://doi.org/10.1039/c3ra42540a

[81] M.K. Devaraju, T. Tomai, I. Honma, Supercritical hydrothermal synthesis of rod like Li_2FeSiO_4 particles for cathode application in lithium ion batteries, Electrochim. Acta 109 (2013) 75–81, https://doi.org/10.1016/j.electacta.2013.07.056

[82] M.K. Devaraju, I. Honma, One-pot synthesis of Li_2FePO_4F nanoparticles via a supercritical fluid process and characterization for application in lithium-ion batteries, RSC Adv. 3 (2013) 19849–19852, https://doi.org/10.1039/c3ra42686f

[83] D.M. Kempaiah, D. Rangappa, I. Honma, Controlled synthesis of nanocrystalline Li_2MnSiO_4 particles for high capacity cathode application in lithium-ion batteries, Chem. Commun. 48 (2012) 2698–2700, https://doi.org/10.1039/c2cc17234h

[84] D. Rangappa, K.D. Murukanahally, T. Tomai, A. Unemoto, I. Honma, Ultrathin nanosheets of Li_2MSiO_4 (M = Fe, Mn) as high-capacity Li-ion battery electrode, Nano Lett. 12 (2012) 1146–1151, https://doi.org/10.1021/nl202681b

[85] M.K. Devaraju, Q.D. Truong, T. Tomai, I. Honma, Supercritical fluid methods for synthesizing cathode materials towards lithium ion battery applications, RSC Adv. 4 (2014) 27452–27470, https://doi.org/10.1039/c4ra01772b

[86] M.K. Devaraju, Q.D. Truong, T. Tomai, H. Hyodo, Y. Sasaki, I. Honma, Antisite defects in $LiCoPO_4$ nanocrystals synthesized via a supercritical fluid process, RSC Adv. 4 (2014) 52410–52414, https://doi.org/10.1039/c4ra10689j

[87] Q.D. Truong, M.K. Devaraju, Y. Ganbe, T. Tomai, I. Honma, Controlling the shape of $LiCoPO_4$ nanocrystals by supercritical fluid process for enhanced energy storage properties, Sci. Rep. 4 (2014) 1–8, https://doi.org/10.1038/srep03975

[88] T. Kozawa, K. Fukuyama, A. Kondo, M. Naito, Wet milling synthesis of $NH_4CoPO_4{\cdot}H_2O$ platelets: formation reaction, growth mechanism, and conversion into high-voltage $LiCoPO_4$ cathode for Li-ion batteries, Mater. Res. Bull. 135 (2021) 111149, https://doi.org/10.1016/j.materresbull.2020.111149

[89] R. Jiang, C. Cui, H. Ma, H. Ma, T. Chen, Study on the enhanced electrochemical performance of $LiMn_2O_4$ cathode material at 55°C by the nano Ag-coating, J. Electroanal. Chem. 744 (2015) 69–76, https://doi.org/10.1016/j.jelechem.2015.02.016

[90] F. Wu, J. Liu, L. Li, X. Zhang, R. Luo, Y. Ye, R. Chen, Surface modification of Li-rich cathode materials for lithium-ion batteries with a PEDOT:PSS conducting polymer, ACS Appl. Mater. Interfaces 8 (2016) 23095–23104, https://doi.org/10.1021/acsami.6b07431

[91] W. Li, J. Hwang, W. Chang, H. Setiadi, K.Y. Chung, J. Kim, Ultrathin and uniform carbon-layer-coated hierarchically porous $LiFePO_4$ microspheres and their electrochemical performance, J. Supercrit. Fluids 116 (2016) 164–171, https://doi.org/10.1016/j.supflu.2016.05.007

[92] A. Örnek, An impressive approach to solving the ongoing stability problems of $LiCoPO_4$ cathode: Nickel oxide surface modification with excellent core–shell principle, J. Power Sources 356 (2017) 1–11, https://doi.org/10.1016/j.jpowsour.2017.04.074

[93] Z. Ma, Y. Peng, G. Wang, Y. Fan, J. Song, T. Liu, X. Qin, G. Shao, Enhancement of electrochemical performance for $LiFePO_4$ cathodes via hybrid coating with electron conductor carbon and lithium ion conductor $LaPO_4$, Electrochim. Acta 156 (2015) 77–85, https://doi.org/10.1016/j.electacta.2015.01.015

[94] G.X. Wang, L. Yang, Y. Chen, J.Z. Wang, S. Bewlay, H.K. Liu, An investigation of polypyrrole-$LiFePO_4$ composite cathode materials for lithium-ion batteries, Electrochim. Acta 50 (2005) 4649–4654, https://doi.org/10.1016/j.electacta.2005.02.026

[95] B. Xiao, X. Sun, Surface and subsurface reactions of lithium transition metal oxide cathode materials: an overview of the fundamental origins and remedying approaches, Adv. Energy Mater. 8 (2018) 1–27, https://doi.org/10.1002/aenm.201802057

[96] P.S. Herle, B. Ellis, N. Coombs, L.F. Nazar, Nano-network electronic conduction in iron and nickel olivine phosphates, Nat. Mater. 3 (2004) 147–152, https://doi.org/10.1038/nmat1063

[97] K. Zeppenfeld, W. Jeitschko, Magnetic behaviour of Ni_3P, Ni_2P, NiP_3 and the series $Ln_2Ni_{12}P_7$ (Ln=Pr, Nd, Sm, Gd-Lu), Behaviour 54 (1993) 1527–1531, https://doi.org/10.1016/0022-3697(93)90346-S

[98] Y. Maeyoshi, S. Miyamoto, Y. Noda, H. Munakata, K. Kanamura, Effect of organic additives on characteristics of carbon-coated $LiCoPO_4$ synthesized by hydrothermal method, J. Power Sources 337 (2017) 92–99, https://doi.org/10.1016/j.jpowsour.2016.10.106

[99] J. Manzi, S. Brutti, Surface chemistry on $LiCoPO_4$ electrodes in lithium cells: SEI formation and self-discharge, Electrochim. Acta 222 (2016) 1839–1846, https://doi.org/10.1016/j.electacta.2016.11.175

[100] Z. Yang, Y. Dai, S. Wang, J. Yu, How to make lithium iron phosphate better: a review exploring classical modification approaches in-depth and proposing future optimization methods, J. Mater. Chem. A 4 (2016) 18210–18222, https://doi.org/10.1039/C6TA05048D

[101] J. Wu, Z. Li, L. Ju, D. Li, J. Zheng, Y. Xu, Effect of the impurities on electrochemical performance of high-voltage $LiCoPO_4$ electrode, Xiyou Jinshu Cailiao Gongcheng Rare Met. Mater. Eng. 42 (2013) 684–687, https://doi.org/10.1016/s1875-5372(13)60056-9

[102] J. Wang, X. Sun, Olivine $LiFePO_4$: The remaining challenges for future energy storage, Energy Environ. Sci. 8 (2015) 1110–1138, https://doi.org/10.1039/c4ee04016c

[103] F. Wang, J. Yang, Y. Nuli, J. Wang, Novel hedgehog-like 5 V $LiCoPO_4$ positive electrode material for rechargeable lithium battery, J. Power Sources 196 (2011) 4806–4810, https://doi.org/10.1016/j.jpowsour.2011.01.055

[104] J. Ni, H. Wang, L. Gao, L. Lu, A high-performance $LiCoPO_4$/C core/shell composite for Li-ion batteries, Electrochim. Acta 70 (2012) 349–354, https://doi.org/10.1016/j.electacta.2012.03.080

[105] A. Örnek, A. Yeşildağ, M. Can, S. Aktürk, A practical and effective strategy for the thin and uniform carbon layer onto $LiCoPO_4$ cathode surface in terms of the rate capability and cycle stability, Mater. Res. Bull. 83 (2016) 1–11, https://doi.org/10.1016/j.materresbull.2016.04.019

[106] P.R. Kumar, V. Madhusudhan Rao, B. Nageswararao, M. Venkateswarlu, N. Satyanarayana, Enhanced electrochemical performance of carbon-coated $LiMPO_4$ (M = Co and Ni) nanoparticles as cathodes for high-voltage lithium-ion battery, J. Solid State Electrochem 20 (2016) 1855–1863, https://doi.org/10.1007/s10008-016-3151-5

[107] A. Örnek, M. Can, A. Yeşildağ, Improving the cycle stability of $LiCoPO_4$ nanocomposites as 4.8 V cathode: Stepwise or synchronous surface coating and Mn substitution, Mater. Charact. 116 (2016) 76–83, https://doi.org/10.1016/j.matchar.2016.04.009

[108] A. Sarapulova, D. Mikhailova, L.A. Schmitt, S. Oswald, N. Bramnik, H. Ehrenberg, Disordered carbon nanofibers/$LiCoPO_4$ composites as cathode materials for lithium ion batteries, J. Sol. Gel Sci. Technol. 62 (2012) 98–110, https://doi.org/10.1007/s10971-012-2691-0

[109] S. Rosenberg, A. Hintennach, In situ carbon-coated $LiCoPO_4$ synthesized via a microwave-assisted path, Russ. J. Electrochem. 51 (2015) 305–309, https://doi.org/10.1134/S1023193515040102

[110] L. Dimesso, C. Spanheimer, W. Jaegermann, Y. Zhang, A.L. Yarin, $LiCoPO_4$ - 3D carbon nanofiber composites as possible cathode materials for high voltage applications, Electrochim. Acta 95 (2013) 38–42, https://doi.org/10.1016/j.electacta.2013.02.002

[111] S. Konishi, D. Murayama, A. Itadani, K. Uematsu, K. Toda, M. Sato, N. Arimitsu, T. Aoki, T. Yamaguchi, Improvement in electrochemical performance of $LiCoPO_4$/C using furnace blacks with high surface areas as a carbon-based composite material, Electrochemistry 85 (2017) 643–646, https://doi.org/10.5796/electrochemistry.85.643

[112] J. Wolfenstine, J. Read, J.L. Allen, Effect of carbon on the electronic conductivity and discharge capacity $LiCoPO_4$, J. Power Sources 163 (2007) 1070–1073, https://doi.org/10.1016/j.jpowsour.2006.10.010

[113] K. Gangulibabu, D. Nallathamby, M. Meyrick, Minakshi, Carbonate anion controlled growth of $LiCoPO_4$/C nanorods and its improved electrochemical behavior, Electrochim. Acta 101 (2013) 18–26, https://doi.org/10.1016/j.electacta.2012.09.115

[114] Y. Hou, K. Chang, B. Li, H. Tang, Z. Wang, J. Zou, H. Yuan, Z. Lu, Z. Chang, Highly [010]-oriented self-assembled $LiCoPO_4$/C nanoflakes as high-performance cathode for lithium ion batteries, Nano Res. 11 (2018) 2424–2435, https://doi.org/10.1007/s12274-017-1864-0

[115] Y. Li, I. Taniguchi, Synthesis and characterization of carbon coated $LiCoPO_4$ as cathode materials for lithium ion batteries, ECS Trans. 85 (2018) 247–258, https://doi.org/10.1149/08513.0247ecst

[116] Y. Yu, H. Zhao, Y. Chen, Z. Feng, X. Liu, H. Yang, Double carbon coated $LiCoPO_4$ nano composite as high-performance cathode for lithium ion batteries, Trends Renew. Energy 6 (2020) 1–11, https://doi.org/10.17737/tre.2020.6.1.00108

[117] A. Örnek, M.Z. Kazancioglu, A novel and effective strategy for producing core-shell $LiNiPO_4$/C cathode material for excellent electrochemical stability using a long-time and low-level microwave approach, Scr. Mater. 122 (2016) 45–49, https://doi.org/10.1016/j.scriptamat.2016.05.022

[118] L. Dimesso, C. Spanheimer, W. Jaegermann, Investigation on graphitic carbon foams - $LiNi_yPO_4$ (y = 0.8-1.0) composites, Solid State Sci. 14 (2012) 1372–1377, https://doi.org/10.1016/j.solidstatesciences.2012.07.023

[119] A. Örnek, Influences of different reaction mediums on the properties of high-voltage $LiNiPO_4$@C cathode material in terms of dielectric heating efficiency, Electrochim. Acta 258 (2017) 524–534, https://doi.org/10.1016/j.electacta.2017.11.095

[120] S. Brutti, J. Manzi, D. Meggiolaro, F.M. Vitucci, F. Trequattrini, A. Paolone, O. Palumbo, Interplay between local structure and transport properties in iron-doped $LiCoPO_4$ olivines, J. Mater. Chem. A 5 (2017) 14020–14030, https://doi.org/10.1039/c7ta03161k

[121] J.L. Allen, T.R. Jow, J. Wolfenstine, Improved cycle life of Fe-substituted $LiCoPO_4$, J. Power Sources 196 (2011) 8656–8661, https://doi.org/10.1016/j.jpowsour.2011.06.057

[122] A. Rajalakshmi, V.D. Nithya, K. Karthikeyan, C. Sanjeeviraja, Y.S. Lee, R. Kalai Selvan, Physicochemical properties of V^{5+} doped $LiCoPO_4$ as cathode materials for Li-ion batteries, J. Sol. Gel Sci. Technol. 65 (2013) 399–410, https://doi.org/10.1007/s10971-012-2952-y

[123] L.S. Devi, K.V. Babu, B. Madhavilatha, M.S. Reddi, K. Samatha, V. Veeraiah, Structural and electrochemical characterizations of nanostructured olivine $LiNi_{1-x}Co_xPO_4$ (x=0 and 0.5) cathode materials for lithium-ion batteries, South Afr. J. Chem. Eng. 25 (2018) 42–47, https://doi.org/10.1016/j.sajce.2017.12.003

[124] Y. Wang, J. Chen, J. Qiu, Z. Yu, H. Ming, M. Li, S. Zhang, Y. Yang, Cr-substituted $LiCoPO_4$ core with a conductive carbon layer towards high-voltage lithium-ion batteries, J. Solid State Chem. 258 (2018) 32–41, https://doi.org/10.1016/j.jssc.2017.08.039

[125] N.V. Kosova, O.A. Podgornova, I.A. Bobrikov, V.V. Kaichev, A.V. Bukhtiyarov, Approaching better cycleability of $LiCoPO_4$ by vanadium modification, Mater. Sci. Eng. B Solid-State Mater. Adv. Technol. 213 (2016) 105–113, https://doi.org/10.1016/j.mseb.2016.04.013

[126] P. Taddesse, A. Berie, K.V. Babu, Effect of Al dopant on the structure, electrical and dielectric properties of olivine LiNi0·5Co0·5PO4 cathode material, J. Mol. Struct. 1219 (2020) 128593, https://doi.org/10.1016/j.molstruc.2020.128593

[127] D. Zhang, J. Zhou, J. Chen, B. Xu, W. Qin, C. Chang, Rapid synthesis of $LiCo_{1-x}Fe_xPO_4$/C cathodes via microwave solvothermal method for Li-ion batteries, Int. J. Electrochem. Sci. 13 (2018) 2544–2555, https://doi.org/10.20964/2018.03.61

[128] D. Di Lecce, R. Brescia, A. Scarpellini, M. Prato, J. Hassoun, A high voltage olivine cathode for application in lithium-ion batteries, ChemSusChem 9 (2016) 223–230, https://doi.org/10.1002/cssc.201501330

[129] J. Wolfenstine, Electrical conductivity of doped $LiCoPO_4$, J. Power Sources 158 (2006) 1431–1435, https://doi.org/10.1016/j.jpowsour.2005.10.072

[130] J.L. Allen, J.L. Allen, T. Thompson, S.A. Delp, J. Wolfenstine, T.R. Jow, Cr and Si substituted-$LiCo_{0.9}Fe_{0.1}PO_4$: structure, full and half Li-ion cell performance, J. Power Sources 327 (2016) 229–234, https://doi.org/10.1016/j.jpowsour.2016.07.055

[131] D. Di Lecce, V. Gancitano, J. Hassoun, Investigation of Mn and Fe substitution effects on the characteristics of high-voltage $LiCo_{1-x}M_xPO_4$ (x = 0.1, 0.4) cathodes prepared by sol-gel route, ACS Sustain. Chem. Eng. 8 (2020) 278–289, https://doi.org/10.1021/acssuschemeng.9b05325

[132] W. Li, B. Song, A. Manthiram, High-voltage positive electrode materials for lithium-ion batteries, Chem. Soc. Rev. 46 (2017) 3006–3059, https://doi.org/10.1039/c6cs00875e

[133] T.Q. Tan, R.A.M. Osman, M.V. Reddy, Z. Jamal, M.S. Idris, Structural and electrical studies of olivine $LiNi_{1-x}(Co_{0.5}Mn_{0.5})_xPO_4$ ($0 \le x \le 1$) at high temperature, Ionics Kiel. 24 (2018) 3733–3744, https://doi.org/10.1007/s11581-018-2536-0

[134] F.C. Strobridge, H. Liu, M. Leskes, O.J. Borkiewicz, K.M. Wiaderek, P.J. Chupas, K.W. Chapman, C.P. Grey, Unraveling the complex delithiation mechanisms of olivine-type cathode materials, $LiFe_xCo_{1-x}PO_4$, Chem. Mater. 28 (2016) 3676–3690, https://doi.org/10.1021/acs.chemmater.6b00319

[135] K.J. Kreder, A. Manthiram, Vanadium-substituted $LiCoPO_4$ core with a monolithic $LiFePO_4$ shell for high-voltage lithium-ion batteries, ACS Energy Lett. 2 (2017) 64–69, https://doi.org/10.1021/acsenergylett.6b00496

[136] F. Wang, J. Yang, Y. NuLi, J. Wang, Highly promoted electrochemical performance of 5 V $LiCoPO_4$ cathode material by addition of vanadium, J. Power Sources 195 (2010) 6884–6887, https://doi.org/10.1016/j.jpowsour.2010.04.071

[137] G. Pagot, F. Bertasi, G. Nawn, E. Negro, G. Carraro, D. Barreca, C. Maccato, S. Polizzi, V. Di Noto, High-performance olivine for lithium batteries: effects of Ni/Co doping on the properties of $LiFe_xNi_pCo_yPO_4$ cathodes, Adv. Funct. Mater. 25 (2015) 4032–4037, https://doi.org/10.1002/adfm.201501167

[138] D. Di Lecce, J. Manzi, F.M. Vitucci, A. De Bonis, S. Panero, S. Brutti, Effect of the iron doping in $LiCoPO_4$ cathode materials for lithium cells, Electrochim. Acta 185 (2015) 17–27, https://doi.org/10.1016/j.electacta.2015.10.107

[139] S. Karthikprabhu, K. Karuppasamy, D. Vikraman, K. Prasanna, T. Maiyalagan, A. Nichelson, A. Kathalingam, H.S. Kim, Electrochemical performances of $LiNi_{1-x}Mn_xPO_4$ (x = 0.05–0.2) olivine cathode materials for high voltage rechargeable lithium ion batteries, Appl. Surf. Sci. 449 (2018) 435–444, https://doi.org/10.1016/j.apsusc.2017.12.060

[140] K. Vijaya Babu, L. Seeta Devi, V. Veeraiah, K. Anand, Structural and dielectric studies of $LiNiPO_4$ and $LiNi_{0.5}Co_{0.5}PO_4$ cathode materials for lithium-ion batteries, J. Asian Ceram. Soc. 4 (2016) 269–276, https://doi.org/10.1016/j.jascer.2016.05.001

[141] S. Karthickprabhu, D. Vikraman, A. Kathalingam, K. Prasanna, H.S. Kim, K. Karuppasamy, Electrochemical and cycling performance of neodymium (Nd^{3+}) doped $LiNiPO_4$ cathode materials for high voltage lithium-ion batteries, Mater. Lett. 237 (2019) 224–227, https://doi.org/10.1016/j.matlet.2018.11.102

[142] M.H. Alfaruqi, S. Kim, S. Park, S. Lee, J. Lee, J.Y. Hwang, Y.K. Sun, J. Kim, Density functional theory investigation of mixed transition metals in olivine and tavorite cathode materials for Li-Ion batteries, ACS Appl. Mater. Interfaces 12 (2020) 16376–16386, https://doi.org/10.1021/acsami.9b23367

[143] H. Gwon, D.H. Seo, S.W. Kim, J. Kim, K. Kang, Combined first-principle calculations and experimental study on multi-component olivine cathode for lithium rechargeable batteries, Adv. Funct. Mater. 19 (2009) 3285–3292, https://doi.org/10.1002/adfm.200900414

[144] K. Hoang, M. Johannes, Tailoring native defects in $LiFePO_4$: Insights from first-principles calculations, Chem. Mater. 23 (2011) 3003–3013, https://doi.org/10.1021/cm200725j

[145] Y.S. Meng, M.E. Arroyo-De Dompablo, Recent advances in first principles computational research of cathode materials for lithium-ion batteries, Acc. Chem. Res. 46 (2013) 1171–1180, https://doi.org/10.1021/ar2002396

[146] A. Osnis, M. Kosa, D. Aurbach, D.T. Major, Systematic first-principles investigation of mixed transition metal olivine phosphates $LiM_{1-y}M'_yPO_4$ (M/M′ = Mn, Fe, and Co) as cathode materials, J. Phys. Chem. C 117 (2013) 17919–17926, https://doi.org/10.1021/jp402755r

[147] L.M. Yan, J.M. Su, C. Sun, B.H. Yue, Review of the first principles calculations and the design of cathode materials for Li-ion batteries, Adv. Manuf. 2 (2014) 358–368, https://doi.org/10.1007/s40436-014-0086-x

[148] Y.S. Meng, M.E. Arroyo-De Dompablo, First principles computational materials design for energy storage materials in lithium ion batteries, Energy Environ. Sci. 2 (2009) 589–609, https://doi.org/10.1039/b901825e

[149] Y. Ma, Computer simulation of cathode materials for lithium ion and lithium batteries: a review, Energy Environ. Mater. 1 (2018) 148–173, https://doi.org/10.1002/eem2.12017

[150] V. Singh, Y. Gershinsky, M. Kosa, M. Dixit, D. Zitoun, D.T. Major, Magnetism in olivine-type $LiCo_{1-x}Fe_xPO_4$ cathode materials: bridging theory and experiment, Phys. Chem. Chem. Phys. 17 (2015) 31202–31215, https://doi.org/10.1039/c5cp04871k

[151] J. Xu, G. Chen, Effects of doping on the electronic properties of $LiFePO_4$: a first-principles investigation, Phys. B Condens. Matter 405 (2010) 803–807, https://doi.org/10.1016/j.physb.2009.05.035

[152] Z.P. Lin, Y.M. Zhao, Y.J. Zhao, First-principles studies of Mn-doped $LiCoPO_4$, Chin. Phys. B 20 (2011) 2–8, https://doi.org/10.1088/1674-1056/20/1/018201

[153] T. Okumura, T. Takeuchi, H. Kobayashi, Application of $LiCoPO_4$ positive electrode material in all-solid-state lithium-ion battery, Electrochemistry 82 (2014) 906–908, https://doi.org/10.5796/electrochemistry.82.906

[154] I. Kurmanbayeva, L. Rakhymbay, K. Korzhynbayeva, A. Adi, D. Batyrbekuly, A. Mentbayeva, Z. Bakenov, Tetrapropylammonium Hydroxide as a Zinc Dendrite Growth Suppressor for Rechargeable Aqueous Battery, Front. Energy Res. 8 (2020) 1–10, https://doi.org/10.3389/fenrg.2020.599009

[155] M. Minakshi, P. Singh, N. Sharma, M. Blackford, M. Ionescu, Lithium extraction-insertion from/into $LiCoPO_4$ in aqueous batteries, Ind. Eng. Chem. Res. 50 (2011) 1899–1905, https://doi.org/10.1021/ie102267x

[156] S. Kalybekkyzy, A. Mentbayeva, Y. Yerkinbekova, N. Baikalov, M.V. Kahraman, Z. Bakenov, Electrospun 3D structured carbon current collector for Li/S batteries, Nanomaterials Basel Switz. 10 (2020) 745, https://doi.org/10.3390/nano10040745

[157] S. Kalybekkyzy, A. Mentbayeva, M.V. Kahraman, Y. Zhang, Z. Bakenov, Flexible S/DPAN/KB nanofiber composite as binder-free cathodes for Li-S batteries, J. Electrochem. Soc. 166 (2019) A5396–A5402, https://doi.org/10.1149/2.0571903jes

[158] S. Kalybekkyzy, A.F. Kopzhassar, M.V. Kahraman, A. Mentbayeva, Z. Bakenov, Fabrication of uv-crosslinked flexible solid polymer electrolyte with pdms for Li-ion batteries, Polymers Basel 23 (2021) 1–12, https://doi.org/10.3390/polym13010015

[159] N. Tolganbek, A. Mentbayeva, N. Serik, N. Batyrgali, M. Naizakarayev, K. Kanamura, Z. Bakenov, Design and preparation of thin film gel polymer electrolyte for 3D Li-ion battery, J. Power Sources 493 (2021) 229686, https://doi.org/10.1016/j.jpowsour.2021.229686

[160] N. Tolganbek, A. Mentbayeva, B. Uzakbaiuly, K. Kanamura, Z. Bakenov, $Li_{1+x}Al_xTi_{2-x}(PO_4)_3$, NASICON-type solid electrolyte fabrication with different methods, Mater. Today Proc. 25 (2019) 97–100, https://doi.org/10.1016/j.matpr.2019.12.279

[161] N. Tolganbek, Y. Yerkinbekova, A. Khairullin, Z. Bakenov, K. Kanamura, A. Mentbayeva, Enhancing purity and ionic conductivity of NASICON-typed $Li_{1.3}Al_{0.3}Ti_{1.7}(PO_4)_3$ solid electrolyte, Ceram. Int. (2021) 1–8, https://doi.org/10.1016/j.ceramint.2021.03.137